

A TECHNIQUE FOR GENERATING THE REFERENCE SIGNALS FOR A  
SYNCHRONOUS LONGITUDINAL VEHICLE CONTROL SYSTEM

A Thesis

Presented in Partial Fulfillment of the Requirements  
for the Degree Master of Science

by

Ronald Alan Brown, BEE

The Ohio State University  
1971

Approved by



Adviser

Department of Electrical  
Engineering

## ACKNOWLEDGMENTS

The author wishes to express his appreciation to his adviser, Professor R. E. Fenton, for his assistance and guidance during the course of this study. Thanks are also extended to Professor K. W. Olson for his invaluable assistance with the physical limitations of electronic equipment.

Thanks are extended to J. Houston for drafting the enclosed figures, and to D. Siekierski for her patience and excellent efforts as as a typist.

Last, but by no means least, the author wishes to express his gratitude for the patience and understanding of his wife and children during the completion of this thesis.

## CONTENTS

	Page
ACKNOWLEDGMENTS	ii
CONTENTS	iii
FIGURES	v
Chapter	
I. INTRODUCTION	1
II. SYNCHRONOUS LONGITUDINAL CONTROL	4
A. Introduction	4
B. Synchronous Control	4
C. Methods of Implementing a Synchronous System	7
D. Derivation of Control Signals	10
E. Small-Signal Analysis of Control System	19
F. Summary	27
III. A TECHNIQUE FOR GENERATING SYNCHRONOUS CONTROL REFERENCE SIGNALS	28
A. Introduction	28
B. Synchronization Error	28
C. Generation of a Low-Velocity Signal	31
D. Sensitivity Analysis	41
E. A Technique for Generating $f_s$	45
F. Considerations of the Effects of Transient Errors in the Reference Signal	55
G. Summary	62

Chapter	Page
IV. AN OVERVIEW OF BASIC SYSTEM DESIGN	64
A. Introduction	64
B. Transmission Line Considerations	64
C. Receiver Considerations	70
D. Traffic Flow Considerations	74
E. Summary	76
V. SUMMARY AND CONCLUSIONS	78
REFERENCES	81

## FIGURES

Number		Page
1.	Position-time histories of two adjacent vehicles.	5
2.	Position of a lead and following vehicle at uniform time intervals.	8
3.	Basic synchronous longitudinal reference system.	10
4.	Spatial distribution of $s(x, 0)$ .	11
5.	Spectrum of $f(t)$ .	12
6.	Moving sampler.	13
7.	Vehicle velocity control system.	14
8.	Shifted spectrum of $s(t)$ due to sampling.	16
9.	Spectrum of $f(t)$ due to velocity error.	17
10.	Model of vehicle control system.	19
11.	Block-diagram representation of vehicle longitudinal dynamics.	20
12.	Modification of vehicle dynamics.	22

Figures cont'd.

Number	Page
13. Simplified block diagram of modified vehicle dynamics.	23
14. Block diagram of vehicle control system.	24
15. Spatial distribution of traveling wave at two instants in time.	29
16. Standing-wave patterns for open- and short-circuit terminations.	31
17. Two-source method of generating traveling envelope.	33
18. Basic receiver required to recover reference signal.	37
19. Asymptotic spectrum of $G_a(\omega)$ .	38
20. Accuracy required of $f_g$ and $r$ to maintain less than 1% velocity error from each parameter.	46
21. Digital frequency synthesizer.	46
22. Two pulse trains showing phase error.	51
23. Cycle skipping of controlled signal due to large phase disturbance.	52
24. Sampling time error due to skipped pulses.	53
25. Majority-logic generation of $f_s$ .	55
26. Alternate model of vehicle control system with noise term.	59

Figures cont'd.

Number	Page
27. Two adjacent transmission links.	67
28. Technique to provide continuity of $g(x, t)$ using separate sampling signals.	69
29. Threshold control of sampling pulses.	69
30. Shielding at junction of two transmission line links.	70
31. Basic receiver required.	73
32. Approximation to constant deceleration.	75
33. Non-synchronous deceleration.	76

## CHAPTER I

### INTRODUCTION

The decade of the sixties has witnessed a tremendous increase in passenger car usage -- as evidenced by a 37% increase in passenger car registrations and a 45% increase in passenger car mileage:<sup>1</sup> However, during this period the total mileage of surfaced highways has increased only 10%. With more than 70% of the designated Interstate and Defense Highway System completed, it is not difficult to foresee that, if the present trends continue, the demand for highway travel will soon far exceed the capacity of the highway system.

It is obvious that meeting the demand for highway travel cannot be achieved by simply building more and larger highways, for the costs are too high -- both in dollars and in the amount of land required. Several public transportation systems, such as High Speed Ground Transportation (HSGT) and rapid transit, have been proposed as solutions to the expected highway problems. It is quite probable that either these or other such approaches will provide a partial solution. However, it is doubtful that a majority of the public will be satisfied with only city-to-city transit via some form of public transportation. For example, in 1969 private automobile travel accounted for 86% of all intercity passenger miles. In comparing automobile travel with alternative modes of public transportation, F. C. Turner, Federal Highway Administrator, has stated:

". . . it is obvious that we should not be thinking or talking about highways versus transit, but instead highways and transit."<sup>2</sup>

In view of these considerations, one satisfactory partial solution would be highway automation, which offers the prospects of both greatly increased lane capacity at high speeds and a reduction in the number of highway accidents.

One important subsystem required by virtually every conceivable type of automated highway system is one for automatic longitudinal control of an individual vehicle. Two general types of control presently appear to be applicable to highway automation -- asynchronous control and synchronous control. The most commonly investigated form of the first of these is a control dependent on the state of the controlled vehicle with respect to the nearest lead vehicle. Bender and Fenton have theoretically analyzed a headway control law and have tested its validity in highway testing using a fully instrumented car.<sup>3,4</sup> They concluded that such a system was practical and safe, but that one must be quite careful in the choice of control constants to ensure asymptotic stability, i.e., perturbations in the lead car velocity must not induce larger perturbations in the velocity of any following cars. The second of these, synchronous control, is most easily visualized by considering an imaginary "conveyor belt" traveling along the highway. This "conveyor belt" moves the vehicles through the highway network to their respective destinations. Weiss<sup>5</sup> has proposed a synchronous control for a capsule transportation system in which the vehicles "chase" computer generated null points along a guideway. Other investigators<sup>6,7,8</sup> have analyzed synchronous control by assuming the vehicles occupy hypothetical "cells" that travel along

the highway. The results of these analyses have indicated there are two major advantages to be gained from a synchronous system:

1. Elimination of instability problems associated with controlling a string of vehicles.
2. Simplification of the problem of merging two strings of vehicles.

However, it should be noted that a secondary control system must be available to detect emergency situations such as a stalled or rapidly decelerating vehicle.

One of the fundamental premises of the research approach taken by the Highway Research Group at The Ohio State University is that an evolutionary development of an automated highway system is mandatory. One possible sequence of developments, similar to that outlined by Plotkin,<sup>9</sup> would use both of the above types of control. In the early development, a vehicle tracker would be used to obtain the relative velocity and headway information required for the Bender-Fenton control law. For the final stage of development, a synchronous control system would become the primary mode of longitudinal control with the previously developed vehicle tracker system becoming a backup mode for emergency control.

The research reported here describes a technique for implementing a synchronous longitudinal control system. Chapter II presents a theoretical analysis of the proposed system and the remaining chapters delineate design specifications for a prototype system.

## CHAPTER II

### SYNCHRONOUS LONGITUDINAL CONTROL

#### A. Introduction

A brief discussion of the theory of synchronous longitudinal control and a technique for generating the required reference signals are presented in this chapter. The basic properties of synchronous control are considered first.

#### B. Synchronous Control

Under normal operating conditions in a synchronous longitudinal control scheme, the vehicles are constrained to follow identical, deterministic position-time histories between any two points in a highway network. In general, due to entrances, exits, merges, and diverges, a vehicle's velocity will not be constant throughout this network, and typical position-time histories requiring a velocity change are shown in Fig. 1. It is important to note that the center-to-center separation between adjacent vehicles would not remain fixed, but instead would be a function of stream speed.

Two important properties of synchronous control, easily derived with the aid of Fig. 1, are:

1. The time separation between adjacent vehicles is constant.

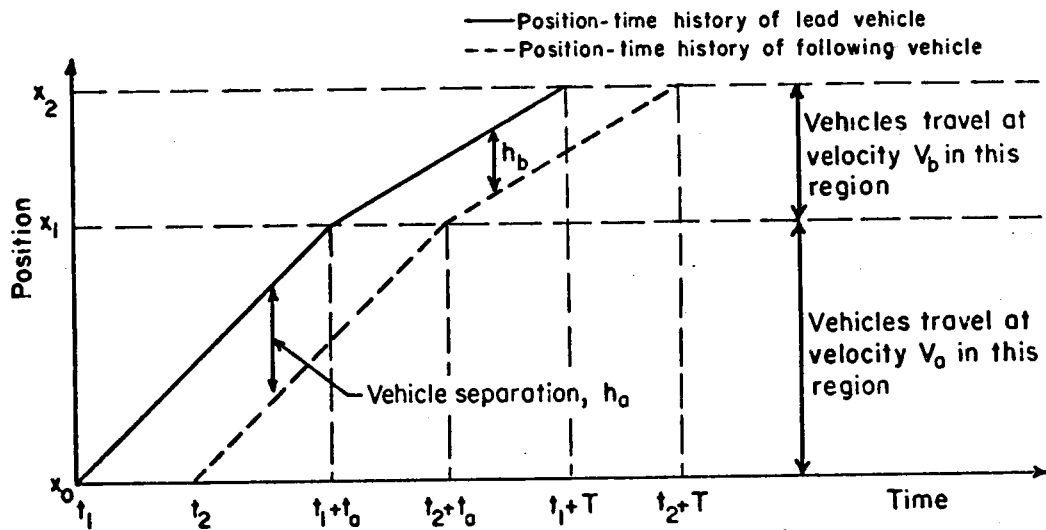


Fig. 1--Position-time histories of two adjacent vehicles.

2. In intervals where adjacent vehicles travel at the same velocity, the separation,  $h$ , defined to include both vehicle length and headway separation, satisfies the following equation:

$$\frac{V_a}{h_a} = \frac{V_b}{h_b} \quad (1)$$

with  $h_a$ ,  $h_b$ ,  $V_a$ , and  $V_b$  as defined in Fig. 1.

Note that Eqn. (1) does not apply for the time interval  $(t_1 + t_a, t_2 + t_a)$  shown in Fig. 1, where both vehicles do not have the same velocity.

The first of the above properties is a direct consequence of the requirement that vehicles follow identical position-time histories, i.e., the position of the second vehicle, as shown in Fig. 1, is delayed  $t_2 - t_1$  seconds relative to the first vehicle. To obtain the second property, let

$p_1(t)$  be the position of the first vehicle

$$p_1(t) = \begin{cases} x_0 + V_a \cdot (t - t_1), & t_1 < t < t_1 + t_a \\ x_1 + V_b \cdot (t - t_1 - t_a), & t_1 + t_a < t < t_1 + T. \end{cases} \quad (2)$$

Similarly, the position of the second vehicle is

$$p_2(t) = \begin{cases} x_0 + V_a \cdot (t - t_2), & t_2 < t < t_2 + t_a \\ x_1 + V_b \cdot (t - t_2 - t_a), & t_2 + t_a < t < t_2 + T. \end{cases} \quad (3)$$

In the interval  $t_2 < t < t_1 + t_a$ , both vehicles maintain a constant velocity  $V_a$  and their separation is

$$\begin{aligned} h_a &= p_1(t) - p_2(t) \\ &= V_a \cdot (t_2 - t_1), \quad t_2 < t < t_1 + t_a. \end{aligned} \quad (4)$$

Similarly, for the interval  $t_2 + t_a < t < t_1 + T$ , one obtains

$$h_b = V_b \cdot (t_2 - t_1), \quad t_2 + t_b < t < t_1 + T. \quad (5)$$

Eliminating  $(t_2 - t_1)$  from Eqns. (4) and (5), the desired relationship is obtained:

$$\frac{V_a}{h_a} = \frac{V_b}{h_b}.$$

The implication of this second property is that the vehicle flow-rate given by

$$p = 3600 \frac{V}{h} \text{ cars/lane/hr}$$

where

$V$  = velocity in ft/sec,

must be constant throughout the entire highway network. It might be possible to relax this constant flow-rate requirement by providing asynchronous "sinks" for redistribution of vehicles between two highway sections with different vehicle flow rates. However, this technique could result in certain vehicles being removed from the traffic stream to await a reduction in travel demand. Driver reaction to such forced removal

might result in severe political problems; however, such considerations are beyond the scope of this paper, and the constant flow-rate requirement will be used in the remainder of this work.

### C. Methods of Implementing a Synchronous System

Theoretically, synchronous control could be achieved by storing a specified position-time history in the memory of an on-board computer and computing the true vehicle position as it traveled along the highway. Comparing the true position with the stored position would then provide a control error value. However, inaccuracies arising from measurement of vehicle velocity or acceleration leads one to conclude that such an autonomous system has little practical value. To overcome the problem of accurately measuring the vehicle velocity, it is necessary to provide a roadside reference signal. The vehicle control system would then be able to determine its position relative to the reference signal and perform any necessary corrections.

One method proposed for generating this roadside reference signal would use discrete position reference points and a constant frequency pulse train.<sup>10</sup> To illustrate how this system would work, consider the position-time histories shown in Fig. 2. The uniform time intervals in this figure represent the constant frequency pulse train and the points  $x_i$  signify positions along the highway at which reference marks would be placed. Note that the positions of the vehicles at each sampling instant would be

$$p_1(i\tau) = x_i, \quad i = 0, 1, \dots, 5, \dots$$

and

$$p_2(i\tau) = x_{i-1}, i = 1, 2, \dots, 6, \dots$$

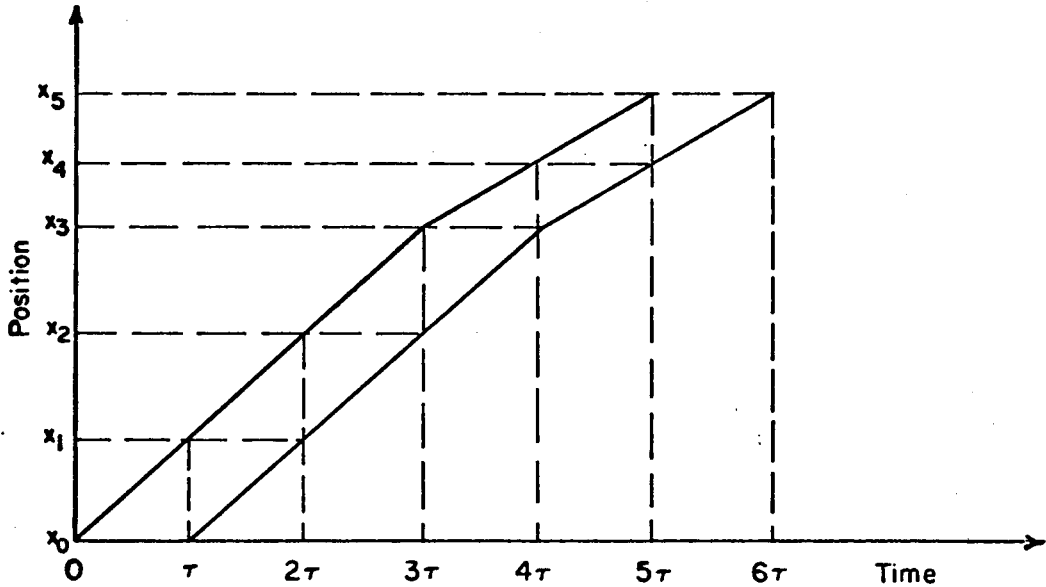


Fig. 2--Position of a lead and following vehicle at uniform time intervals.

As a vehicle departs from the specified position-time history, it will not be directly over a position reference mark at the time a pulse is received. This deviation in position would be the input to the vehicle control system so as to correct the position error. Note from Fig. 2, that when the first vehicle is at reference point  $x_i$ , the second vehicle would be at the immediately preceding reference point  $x_{i-1}$ . To obtain time synchronization it would be necessary to transmit the pulse train from an external source rather than generating it on board each vehicle. Also note from Fig. 2, that vehicle velocity would be controlled by the spacing of the reference points  $x_i$ , thus

$$V_i = \frac{x_{i+1} - x_i}{\tau}$$

where

$V_i$  = average velocity between the points  $x_i$  and  $x_{i+1}$ .

The major difficulty with this technique is the relatively low pulse rate required. As an example, consider a controlled velocity of 100 ft/sec (about 70 mph). Using a reference point spacing of 20 ft. so that a vehicle is in the vicinity of only one reference point at a time, the required pulse rate is only 5 Hz. Considering such factors as roadway slope and external wind forces, it might not be possible to obtain satisfactory operation with such a low position-information rate. However, simply increasing the pulse rate introduces a problem of discriminating between reference points. For example, with a pulse rate of 20 Hz the reference-point spacing would be only 5 ft. Assuming an average vehicle length of 18 ft., a vehicle would then be over 3 or 4 points simultaneously and the possibility would exist that the vehicle would erroneously position itself on the wrong reference point.

In view of the expected problems arising from a discrete reference-point technique, a system using continuous or nearly continuous position information would be desirable. A promising method for obtaining high position-information rates involves the use of a technique similar to the stroboscopic measurement of angular rotation rates. By judiciously sampling a high-velocity traveling wave, its apparent velocity would be much lower. The basic structure of the system, as shown in Fig. 3, would employ a reference sinusoid transmitted along the highway and an external sampling synchronization signal. The controlled vehicles would lock onto

a null point of the low-velocity sampled wave and track it along the highway. The external sampling signal would be required to ensure that all vehicles sample the high-velocity reference wave at the same instant. Vehicle spacing would be controlled by the wavelength of the reference signal and velocity would be controlled by the sampling rate as is described in subsequent sections.

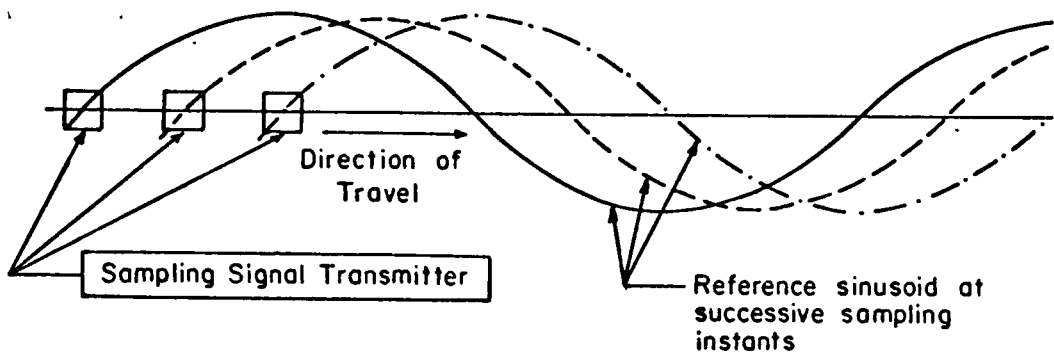


Fig. 3--Basic synchronous longitudinal reference system.

#### D. Derivation of Control Signals

The reference signal transmitted along the highway can be expressed as a time-harmonic traveling wave:

$$s(x, t) = B \sin(\omega_R t - \beta_R x) \quad (6)$$

where

$\omega_R$  = frequency of the traveling wave

$\beta_R$  = phase constant.

The phase constant,  $\beta_R$ , is determined from the wavelength of the traveling wave as shown in Fig. 4.

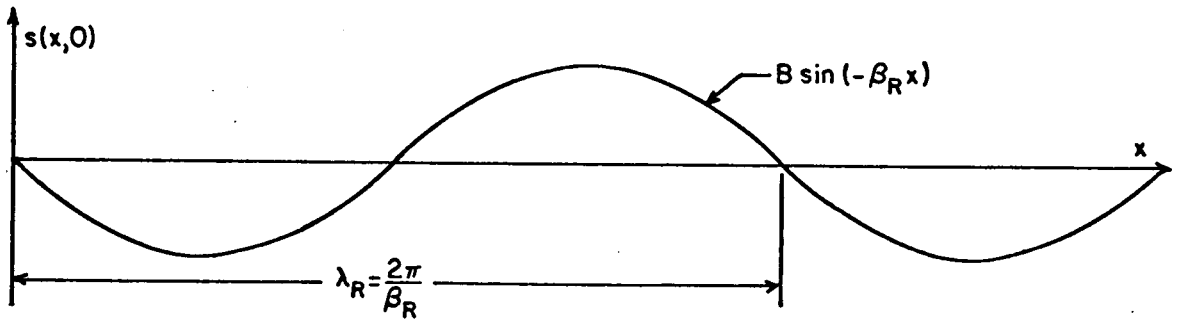


Fig. 4--Spatial distribution of  $s(x, 0)$ .

Sampling the traveling wave at the point  $x = 0$ , produces the function:

$$f(t) = \sum_{-\infty}^{\infty} B \sin(n\omega_R T_s) \delta(t - nT_s) \quad (7)$$

where

$\delta(t)$  = impulse function,

$T_s$  = sampling period.

The Fourier transform of  $f(t)$  is<sup>11</sup>

$$F(\omega) = \frac{1}{T_s} \sum_{-\infty}^{\infty} S(\omega + n\omega_s) \quad (8)$$

where

$S(\omega)$  = Fourier transform of  $s(0, t)$

$\omega_s$  =  $2\pi/T_s$ .

Note that the spectrum of  $f(t)$  is simply  $S(\omega)$  shifted by all integer multiples of  $\omega_s$ . The transform of  $s(0, t)$  is

$$S(\omega) = -j\pi B \delta(\omega - \omega_R) + j\pi B \delta(\omega + \omega_R), \quad (9)$$

and the spectrum of  $f(t)$  is shown in Fig. 5. The result shown in this figure implicitly assumes that:

$$|\omega_R - (k+1)\omega_s| > |\omega_R - k\omega_s|$$

where

$$k = \text{greatest integer of } \omega_R/\omega_s ,$$

or equivalently:

$$-\omega_R + (k+1)\omega_s > \omega_R - k\omega_s > 0 . \quad (10)$$

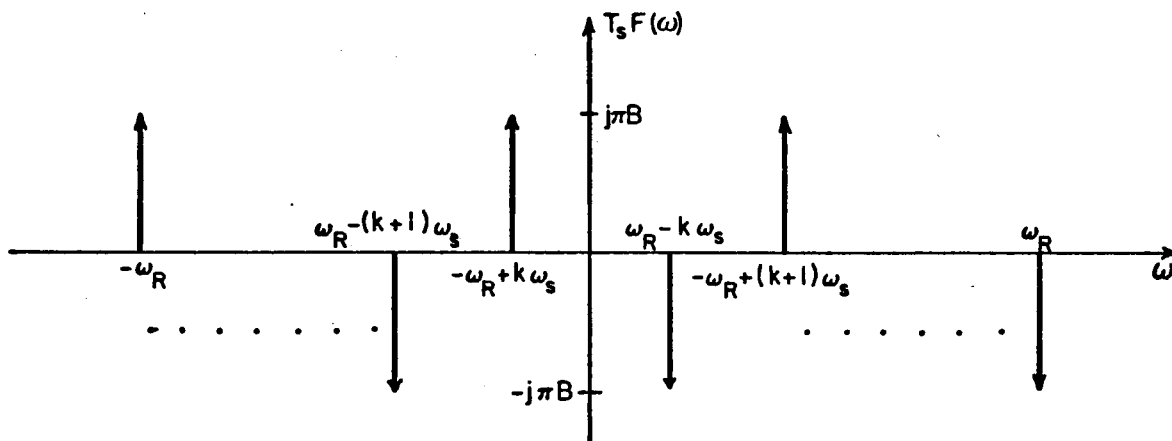


Fig. 5--Spectrum of  $f(t)$ .

From Eqn. (10), one obtains

$$\omega_R > k\omega_s , \quad (11a)$$

and

$$\frac{\omega_s}{2} > \omega_R - k\omega_s . \quad (11b)$$

Note from Fig. 5 and Eqn. (11b), that only the impulses at

$$\omega = \pm(\omega_R - k\omega_s)$$

appear in  $F(\omega)$  for

$$|\omega| < \frac{\omega_s}{2}.$$

Thus, if one were to use a low-pass filter with cut-off frequency  $\omega_s/2$ , the output spectrum would be

$$F_1(\omega) = -j\pi\frac{B}{T_s} \delta(\omega - \omega_R + k\omega_s) + j\pi\frac{B}{T_s} \delta(\omega + \omega_R - k\omega_s). \quad (12)$$

Taking the inverse transform of Eqn. (12):

$$f_1(t) = \frac{B}{T_s} \sin(\omega_R - k\omega_s)t. \quad (13)$$

Eqn. (13) represents the low-pass output of a sampler stationary at the point  $x = 0$ . To determine the phase velocity of this output, let the sampler be moving in the positive  $x$  direction with velocity  $V$ . The corresponding block diagram is shown in Fig. 6.

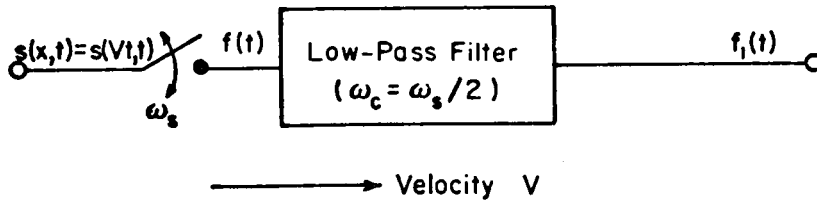


Fig. 6--Moving sampler.

Using  $x(t) = Vt$  in Eqn. (6), the input is

$$s(Vt, t) = s(t) = B \sin [ (\omega_R - \beta_R V)t ], \quad (14)$$

which is of the same form as the stationary case with  $\omega_R$  replaced by  $\omega_R - \beta_R V$ . Thus, from Eqn. (13) the output is

$$f_1(t) = \frac{B}{T_s} \sin(\omega_R - \beta_R V - k\omega_s)t. \quad (15)$$

The apparent phase velocity of  $s(x, t)$  is obtained from Eqn. (15) by setting  $f_1(t) = 0$ , thus

$$V_R^* = \frac{\omega_R - k\omega_s}{\beta_R} \quad (16)$$

Note that the apparent velocity of the output can be adjusted to any arbitrary value by a proper choice of  $\omega_s$ . This result suggests that the desired vehicle velocity could be obtained by having the vehicle track a "constant" phase point of  $f_1(t)$  (The suggested approach is outlined in Fig. 7).

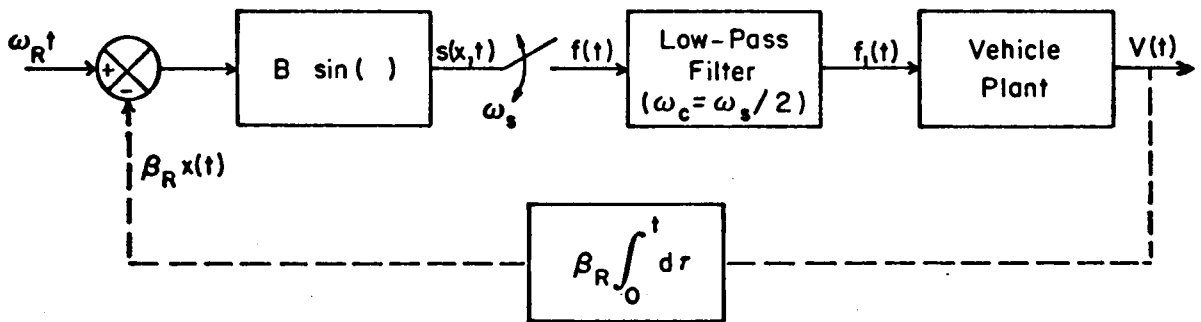


Fig. 7--Vehicle velocity control system.

The feedback shown in this figure results from the relative motion of the vehicle with respect to the traveling reference signal.

To obtain the filtered error signal,  $f_1(t)$ , let the vehicle velocity be:

$$x(t) = V_R^* - e(t) \quad (17)$$

where

$$V_R^* = \text{reference velocity given by Eqn. (16)}$$

$$e(t) = \text{velocity error.}$$

The corresponding vehicle position is

$$x(t) = x_0 + V_R^* t - \int_0^t e(\tau) d\tau. \quad (18)$$

From Eqn. (6), the input to the sampling device is

$$s(x(t), t) = B \sin [(\omega_R - \beta_R V_R^*)t - \beta_R (x_0 - \int_0^t e(\tau) d\tau)]. \quad (19)$$

Expanding Eqn. (19):

$$s(x(t), t) = s(t) = g_1(t) \sin (\omega_R - \beta_R V_R^*)t + g_2(t) \cos (\omega_R - \beta_R V_R^*)t \quad (20)$$

where

$$g_1(t) = B \cos (\beta_R x_0 - \beta_R \int_0^t e(\tau) d\tau)$$

$$g_2(t) = -B \sin (\beta_R x_0 - \beta_R \int_0^t e(\tau) d\tau).$$

The Fourier transform of  $s(t)$  is

$$S(\omega) = \begin{cases} \frac{1}{2j} G_1(\omega - \omega_R + \beta_R V_R^*) + \frac{1}{2} G_2(\omega - \omega_R + \beta_R V_R^*), & \omega > 0 \\ -\frac{1}{2j} G_1(\omega + \omega_R - \beta_R V_R^*) + \frac{1}{2} G_2(\omega + \omega_R - \beta_R V_R^*), & \omega < 0 \end{cases} \quad (21)$$

where  $G_1(\omega)$  and  $G_2(\omega)$  are the Fourier transforms of  $g_1(t)$  and  $g_2(t)$ , respectively.

Let

$$S(\omega) = S_+(\omega) + S_-(\omega)$$

where  $S_+(\omega)$  and  $S_-(\omega)$  denote the spectrum of  $s(t)$  for positive and negative frequencies, respectively. Referring to Fig. 5, one obtains the spectrum shown in Fig. 8. (Here, for the sake of convenience, both  $S_+(\omega)$  and  $S_-(\omega)$  are represented as triangular, band-limited spectra). From Eqn. (21)

$$S_+(\omega + k\omega_s) = \frac{1}{2j} G_1(\omega + \omega_R - \beta_R V_R^* + k\omega_s)$$

$$+ \frac{1}{2} G_2(\omega + \omega_R - \beta_R V_R^* + k\omega_s)$$

Suspected no page 16

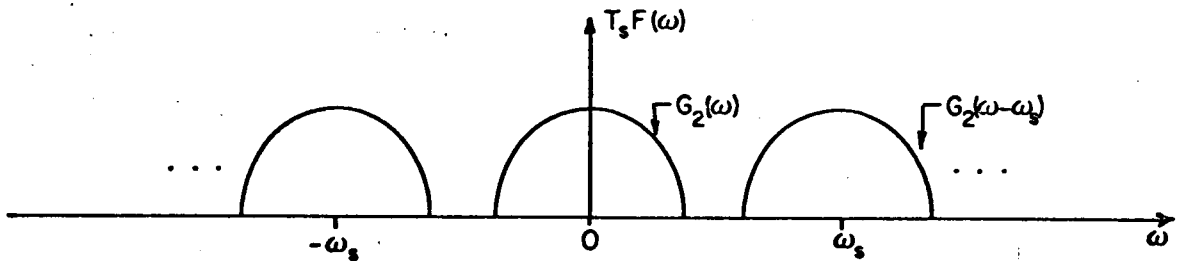


Fig. 9--Spectrum of  $f(t)$  due to velocity error.

and

$$f_1(t) = -\frac{B}{T_s} \sin \left( \beta_R x_0 - \beta_R \int_0^t e(\tau) d\tau \right). \quad (25)$$

It will be shown later that the above assumption concerning the bandwidth of  $G_2(\omega)$  is valid.

Referring to Fig. 7, one sees that when the vehicle is traveling at the reference velocity,  $V_R^*$ , the error signal,  $f_1(t)$ , should be zero. Assuming no velocity error, the only points at which  $f_1(t)$ , given by Eqn. (25), can be zero correspond to an initial vehicle position satisfying

$$\beta_R x_0 = n\pi, \quad n = 0, \pm 1, \pm 2, \dots \quad (26)$$

From Fig. 4 4

$$\beta_R = \frac{2\pi}{\lambda_R}$$

where

$$\lambda_R = \text{wavelength of the reference signal}$$

thus

$$x_0 = \frac{n}{2} \lambda_R, \quad n = 0, \pm 1, \pm 2, \dots \quad (27)$$

and a string of vehicles, positioned for zero-error signal, will be spaced some integer multiple of  $\lambda_R/2$ . However, the use of a linear vehicle control system causes one-half of the points defined by Eqn. (27) to be unstable as can be seen from the following argument:

Consider a small displacement,  $\delta_x$ , about the point  $x_0 = \lambda_R/2$ . Then, from Eqn. (25)

$$f_1(t) = \frac{B}{T_s} \sin(\pi + \beta_R \delta_x)$$

$$\approx \frac{B}{T_s} \beta_R \delta_x .$$

One sees that a positive displacement produces an increase in the error signal and causes the vehicle to move further in the positive direction. Hence, all points with  $n$  odd in Eqn. (27) are unstable.

With the restriction that  $n$  must be even, Eqn. (26) is modified such that

$$\beta_R x_0 = 2n\pi, \quad n = 0, \pm 1, \pm 2, \dots,$$

and Eqn. (25) simplifies to:

$$f_1(t) = \frac{B}{T_s} \sin\left(\beta_R \int_0^t e(\tau) d\tau\right) . \quad (28)$$

Using the velocity error,  $e(t)$ , obtained from Eqn. (17) in conjunction with Eqn. (28), suggests the model shown in Fig. 10 as a representation of the vehicle control system. In comparing this analytical model with Fig. 7, one sees that the position-feedback,  $x(t)$ , no longer appears explicitly. Note that this is not an inconsistent result since the combination of the sinusoidal nonlinearity and allowable initial position points is equivalent to a zero-input position reference signal.

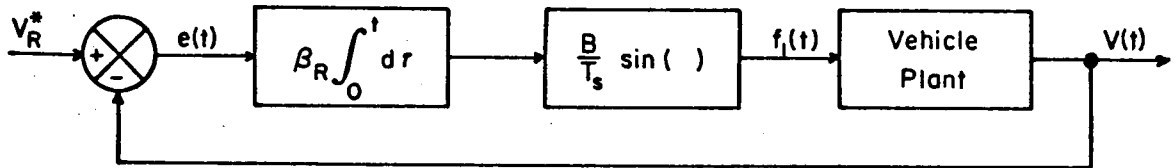


Fig. 10--Model of vehicle control system.

### E. Small-Signal Analysis of Control System

The preceding section described a vehicle control system for which, assuming ideal operating conditions, the steady-state position would be

$$x(t) = n\lambda_R + V_R^* t .$$

To investigate the performance of this system, one must be able to characterize the vehicle response as a function of the controlling signal. A frequently used representation of the vehicle longitudinal dynamics is shown in Fig. 11. The external disturbance force shown in this figure accounts for variations in roadway slope, wind gusts, and other random perturbing forces. From Fig. 11

$$F(A) + f_d = mpV + F_f(V) \quad \left( p = \frac{d}{dt} \right) \quad (29)$$

where

- $F(A)$  = net force applied by the engine-drivetrain combination
- $f_d$  = disturbance force
- $F_f(V)$  = effective drag force

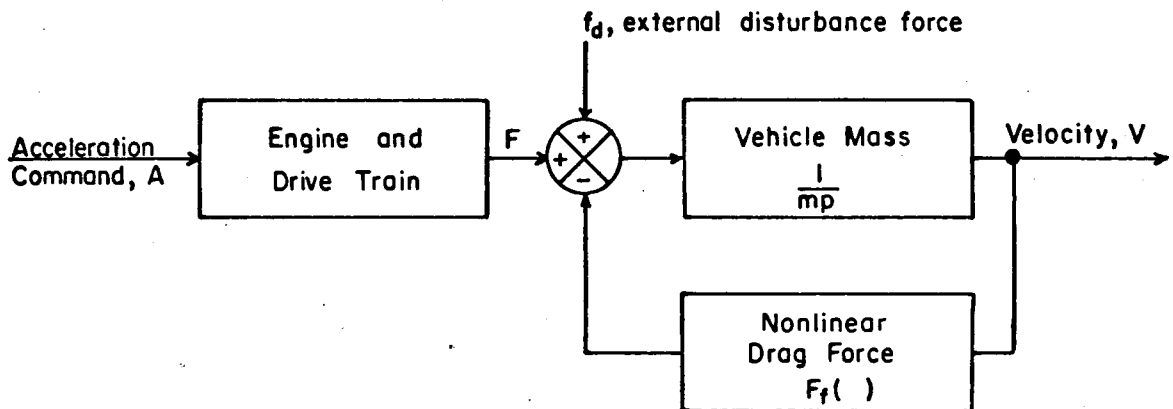


Fig. 11--Block-diagram representation of vehicle longitudinal dynamics.

A = acceleration command

V = velocity of vehicle.

In the situation where a vehicle is traveling at a nearly constant speed  $V_R^*$ , it is convenient to linearize Eqn. (29). To this end, let

$$V = V_R^* + v \quad (30)$$

and

$$A = A_R + a \quad (31)$$

where

v = variational component of vehicle velocity

a = variational component of acceleration command.

Assuming both  $F(A)$  and  $F_f(V)$  can be adequately represented by the first two terms of a Taylor series expansion, then

$$F(A) \approx F(A_R) + G_o a \quad (32)$$

and

$$F_f(V) \approx F_f(V_R^*) + K_f v \quad (33)$$

where

$$G_o = \left. \frac{dF}{dA} \right|_{A = A_R} = \text{incremental engine gain}$$

$$K_f = \left. \frac{dF_f}{dV} \right|_{V = V_R^*} = \text{incremental drag force constant.}$$

Substituting Eqns. (30), (32), and (33) into (29) and noting that for a steady-state constant velocity  $F(A_R) = F_f(V_R^*)$ , one obtains

$$G_o a + f_d = mpv + K_f v. \quad (34)$$

In the absence of external disturbances, Eqn. (34) may be rewritten as

$$v = \frac{K_c}{T_c p + 1} a \quad (35)$$

where

$$K_c = G_o / K_f = \text{vehicle gain}$$

$$T_c = m / K_f = \text{vehicle time constant.}$$

Earlier experimental work<sup>12</sup> has shown that the parameters  $K_c$  and  $T_c$  vary considerably with velocity, roadway slope, external wind forces, and road surface. Such variations were partially overcome by using internal feedback with a gain of  $\delta$  as shown in Fig. 12. From this figure

$$G_o(a - \delta v) + f_d = mpv + K_f v,$$

thus

$$v = \frac{G_o}{mp + K_f + \delta G_o} \left( a + \frac{f_d}{G_o} \right). \quad (36)$$

The operator in Eqn. (36) can be rearranged as follows

$$\frac{G_o}{mp + K_f + \delta G_o} = \frac{G_o / K_f}{\frac{m}{K_f} p + 1 + \frac{\delta G_o}{K_f}}$$

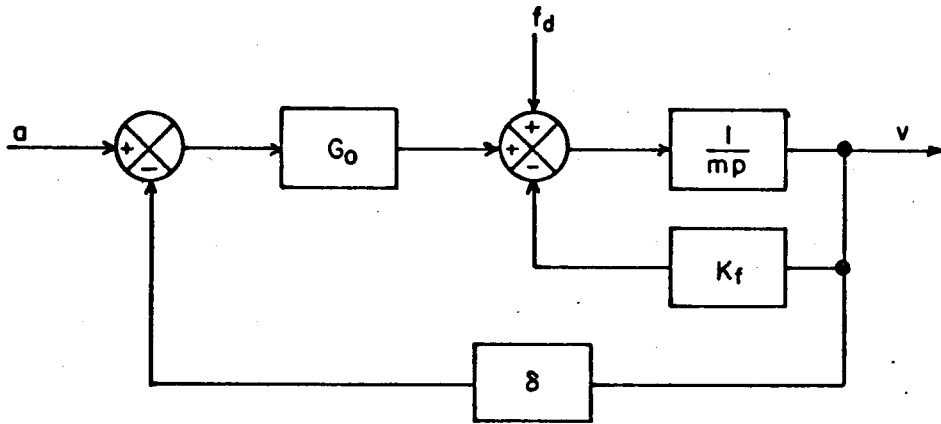


Fig. 12--Modification of vehicle dynamics.

$$= \frac{K_o}{T_o p + 1} \quad (37)$$

where

$$K_o = \frac{K_c}{1 + \delta K_c}$$

$$T_o = \frac{T_c}{1 + \delta K_c}$$

Note that the effect of parameter changes has been reduced by the factor

$$\frac{1}{1 + \delta K_c}$$

It is convenient to modify the term containing the disturbance force in Eqn. (36) as follows

$$\frac{f_d}{G_o} = \frac{f_d}{m} \frac{m}{K_f} \frac{K_f}{G_o}$$

$$= \frac{f_d}{m} \frac{T_c}{K_c}$$

$$\frac{f_d}{G_o} = \frac{f_d}{m} \frac{T_o}{K_o} \quad (38)$$

Substituting Eqns. (37) and (38) for the respective terms in Eqn. (36), one obtains

$$v = \frac{K_o}{T_o p + 1} \left( a + \frac{f_d}{m} \frac{T_o}{K_o} \right) . \quad (39)$$

The block diagram representing Eqn. (39) is shown in Fig. 13.

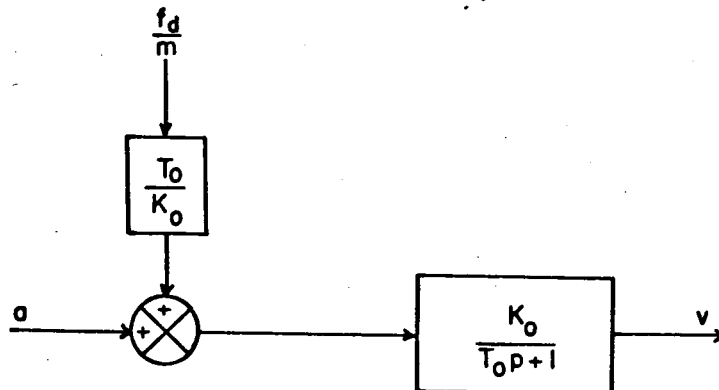


Fig. 13--Simplified block diagram of modified vehicle dynamics.

Assuming the vehicle dynamics are adequately represented by the block diagram in Fig. 13, then one may simply replace the vehicle plant in Fig. 10 with this diagram. Before making this substitution however, note that for small signals, the sinusoid nonlinearity in Fig. 10 may be replaced by a linear approximation

$$\sin \phi \approx \phi$$

which is fairly accurate for  $\phi < 0.3$  rad. Taking the Laplace transform of the equations representing the vehicle dynamics and control system, and using the linear approximation for  $\sin \phi$ , one obtains the block diagram in Fig. 14. Note that this diagram is based on velocity variation about the steady-state value  $V_R^*$ , hence  $R(s) = 0$ . The gain factor  $K$  shown in this

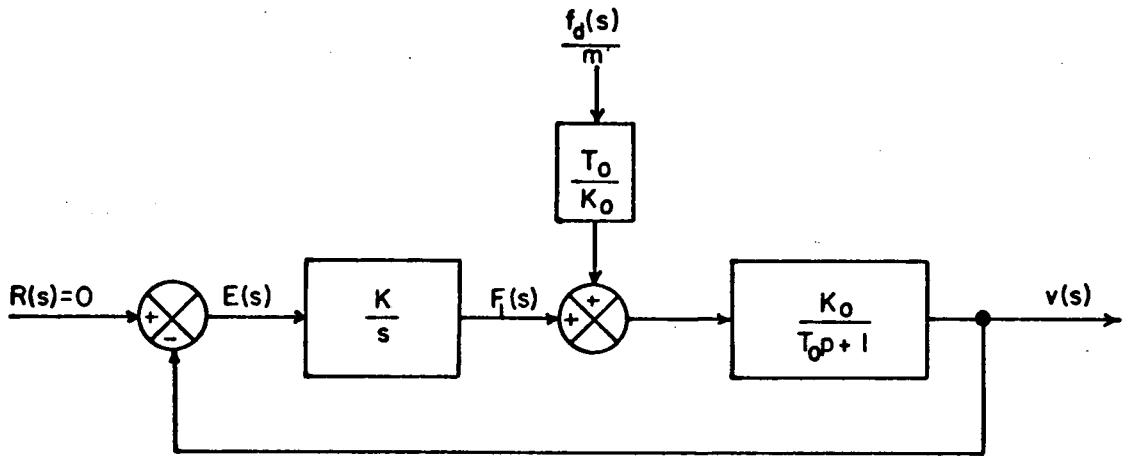


Fig. 14--Block diagram of vehicle control system.

figure is

$$K = \beta_R \frac{B}{T_s} .$$

To examine the performance of the system shown in Fig. 14, two cases must be considered:

1. The transient response due to a command to change velocity.
2. The transient response due to expected disturbance forces.

The first of these will be examined in a subsequent chapter and only the second case will be discussed at this point.

The transform of the vehicle position error is

$$X_e(s) = \frac{v(s)}{s} .$$

From Fig. 14,

$$\begin{aligned} F_1(s) &= \frac{K}{s} E(s) \\ &= -\frac{K}{s} v(s) \end{aligned} \tag{40}$$

and

$$X_e(s) = -\frac{F_1(s)}{K},$$

thus, the transfer function of interest is

$$\frac{X_e(s)}{f_d(s)/m} = -\frac{F_1(s)}{\frac{K}{m} f_d(s)}. \quad (41)$$

From Fig. 14

$$v(s) = F_1(s) + \frac{T_o}{K_o} \frac{f_d(s)}{m} \frac{K_o}{T_o s + 1},$$

and with Eqns. (40) and (41) one obtains

$$\frac{X_e(s)}{f_d(s)/m} = \frac{T_o}{T_o s^2 + s + KK_o}. \quad (42)$$

It is convenient to obtain Eqn. (42) in the standard form for a second-order system

$$\frac{X_e(s)}{f_d(s)/m} = \frac{1}{s^2 + 2\zeta\omega_n s + \omega_n^2} \quad (43)$$

where

$$\omega_n^2 = \frac{KK_o}{T_o}$$

$$\zeta = \frac{1}{2\sqrt{T_o KK_o}}.$$

The position error due to various types of disturbances may be investigated by Eqn. (43); however, the primary disturbance of interest is a constant force arising from a change in roadway slope or a change in wind velocity. For this case

$$\frac{f_d(s)}{m} = \frac{\alpha_d}{s} \quad (44)$$

where

$\alpha_d$  = magnitude of acceleration disturbance.

The steady-state position error introduced by this force is easily obtained by using the final value theorem for Laplace transforms

$$\lim_{t \rightarrow \infty} x_e(t) = \lim_{s \rightarrow 0} sX_e(s) .$$

Using Eqns. (43) and (44)

$$sX_e(s) = \frac{\alpha_d}{s^2 + 2\zeta\omega_n s + \omega_n^2} ,$$

thus

$$\lim_{t \rightarrow \infty} x_e(t) = \frac{\alpha_d}{\omega_n^2} . \quad (45)$$

Clearly, to reduce the effect of a constant disturbance force, one would wish to obtain a large value for  $\omega_n$ . However, simply increasing  $\omega_n$  leads to a very responsive vehicle and would result in passenger discomfort. In addition to this passenger comfort restraint, there is a further limitation on  $\omega_n$  due to the capabilities of present day vehicles. The effective time constant for a second-order system is

$$\tau = \frac{1}{\zeta\omega_n} . \quad (46)$$

This time constant should be chosen such that it may be realized by the majority of automobiles in use on the highways. Currently, it appears that the lower bound on obtainable time constants is between 1 and 2 sec.<sup>13</sup>

Using  $\tau = 2$  sec as a conservative estimate, one obtains from Eqn. (46)

$$\omega_n = \frac{1}{2\zeta} . \quad (47)$$

Choosing  $\zeta = 0.5$  appears to be a reasonable compromise between obtaining a large value of  $\omega_n$  and reducing the oscillatory motion of the transient response, thus

$$\zeta = 0.5$$

and

$$\omega_n = 1 .$$

With  $\omega_n = 1$ , note from Eqn. (45) that an extremely large disturbance of 0.3 g's produces a position error of only 0.3 ft.

On the basis of this analysis, it seems certain that a vehicle position accuracy of at least  $\pm 0.5$  ft could be easily obtained.

#### F. Summary

The basic theory of Synchronous Longitudinal Control has been discussed in this chapter and some possible methods of obtaining synchronous control were considered. A sampled-data system was analyzed in detail and a small-signal model of the system was derived. The two most important properties of this system are:

1. Vehicle speed is controlled by the sampling frequency.
2. Vehicle spacing is controlled by the wavelength of the reference signal.

Some problems associated with this system, such as sampling synchronization error, and a technique for implementing the system are discussed in the next chapter.

## CHAPTER III

### A TECHNIQUE FOR GENERATING SYNCHRONOUS CONTROL REFERENCE SIGNALS

#### A. Introduction

The analysis of the sampled-data synchronous longitudinal control system presented in the previous chapter assumed rather idealistic operating conditions, i.e., perfect synchronization among individual sampling units and zero-error in the reference and sampling frequencies. In this chapter, the performance of the proposed system in the presence of slight errors is investigated and a promising method of implementing the system in a real-world environment is described.

#### B. Synchronization Error

There must necessarily be some small time difference between sampling instants at individual vehicles due to the large physical distances involved. To examine the effect of this synchronization error, consider an R-F signal traveling along the highway at the velocity of light. The spatial distribution of this wave at two instants in time is shown in Fig. 15. The wave-form at time  $t_1 + \tau$  is shifted by a distance

$$\delta_x = c \tau \quad (48)$$

where

$c$  = velocity of light  $\approx 10^9$  ft/sec

$\tau$  = synchronization error.

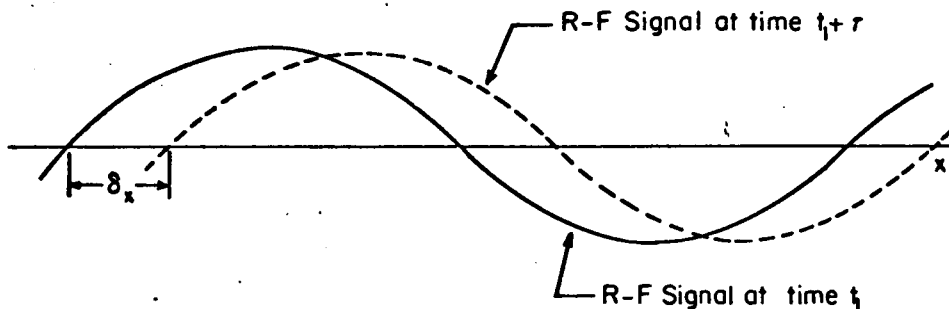


Fig. 15--Spatial distribution of traveling wave at two instants in time.

Since the individual vehicles obtain their position reference from the spatial distribution of the reference signal at each sampling instant, it is clear from Fig. 15 that a synchronization error of  $\tau$  produces an uncertainty in the actual position of each vehicle. Thus, one may only expect the separation between adjacent vehicles to satisfy

$$\lambda - 2 \delta_x < h < \lambda + 2 \delta_x .$$

Overall system safety requirements will determine the allowable position uncertainty; however, other sources of position error, such as wind gusts, produce a cumulative effect on the position error. Hence, it will be necessary to keep the synchronization position error as small as possible. For the sake of illustration, assume that an uncertainty of one foot is tolerable, then from Eqn. (48)

$$\tau < 10^{-9} \text{ sec}$$

Under laboratory conditions, the above synchronization accuracy could be achieved. However, for the desired application, the sampling units would

be separated by several feet and the propagation delay of any known synchronization signal would exceed one nanosecond. Clearly, the straightforward use of an R-F signal as the reference wave is inadequate.

From Eqn. (48) one sees that the allowable synchronization error for a specified maximum position error is inversely proportional to the velocity of the traveling wave; thus, if the traveling wave had a velocity 1/1000 the speed of light, the allowable error would be 1  $\mu$ sec. Assuming the synchronization signal is transmitted at the velocity of light, the time delay between two vehicles 100 ft apart is about 0.1  $\mu$ sec. If other sources of synchronization error are assumed to be negligible compared to the propagation delay, the required synchronization could be obtained by slowing down the reference wave.

One method of slowing down electromagnetic waves uses inductive loading of a transmission line.<sup>14</sup> This technique is used in telephony to reduce transmission distortion and causes phase velocity reductions in the order of 0.1 to 0.01. However, the method used is lumped inductive loading at intervals much less than the carrier wavelength. For the proposed application, the carrier wavelength determines inter-vehicle spacing and would be in the range of 10 to 100 ft to obtain high vehicle flow-rates. Thus, lumped loading at intervals of less than 10 ft would be required. The impracticality of such close spacing and the uncertainty of obtaining a phase velocity reduction in the order of 1/1000 leads one to conclude that this technique would not be satisfactory for the desired application.

In the course of the research reported here, it was found that a traveling signal having an arbitrary phase velocity could be generated. This technique has been extensively investigated and, as will be shown in

the following sections, it appears to provide a satisfactory solution to the problem of synchronization errors.

### C. Generation of a Low-Velocity Signal

To illustrate the basic idea of the technique that would be used to generate a low-velocity signal, consider the standing-wave voltage distribution along a lossless transmission line as shown in Fig. 16. The different standing-wave patterns for open- and short-circuit terminations suggest that some appropriate time variation of the termination impedance,  $Z_R$ , would cause the standing-wave to move with constant velocity from the pattern shown as a solid line in this figure to that shown as a dashed line.

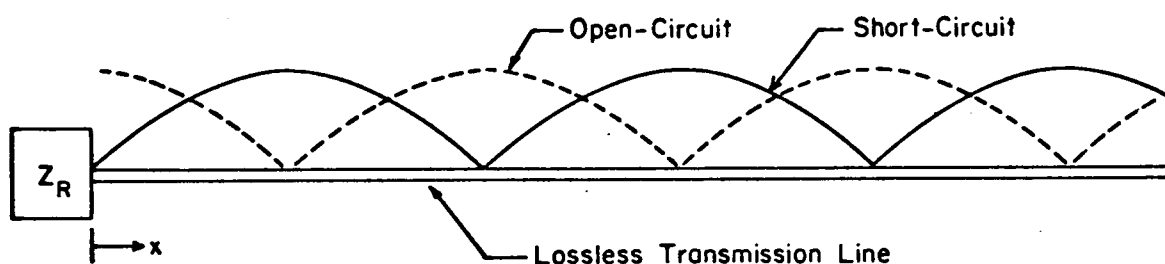


Fig. 16--Standing-wave patterns for open- and short-circuit terminations.

For a lossless termination impedance, the voltage along the line can be expressed as

$$v(x,t) = \text{Re} \left[ V_M \cos \left( \beta x - \frac{\omega t}{2} \right) \exp \left\{ j \left( \omega t + \frac{\omega x}{2} \right) \right\} \right] \quad (49)$$

where

$\text{Re} [ ]$  = real part of complex function

$\theta_K$  = angle of the reflection coefficient at the termination impedance.

The phase velocity of the envelope of  $v(x, t)$  is obtained by taking the time derivative of a constant phase point

$$\frac{d}{dt} (\beta x - \frac{\theta_K}{2}) = 0 ,$$

thus

$$V_p = \frac{1}{2\beta} \frac{d\theta_K}{dt} \quad (50)$$

where

$$V_p = \frac{dx}{dt} = \text{phase velocity of the envelope.}$$

(If  $Z_R$  were constant,  $V_p$  would be zero and a standing-wave pattern would result). The required time variation of  $\theta_K$  to obtain a constant envelope velocity is

$$\theta_K = 2\beta V_p t + \theta_0 . \quad (51)$$

Thus, the time variation of  $Z_R$  could be obtained by varying  $\theta_K$ ; however, a more desirable result is obtained by considering the form of the voltage reflected at the termination. Given the incident voltage

$$v_I(x, t) = \text{Re} [V_I \exp \{j(\omega t + \beta x)\}]$$

the reflected voltage is

$$v_R(x, t) = \text{Re} [V_I R \exp \{j(\omega t - \beta x + \theta_K)\}] , \quad (52)$$

where

$R$  = magnitude of the reflection coefficient at the load.

With  $\theta_K$  as given by Eqn. (51) substituted into Eqn. (52), one obtains

$$v_R(x, t) = \text{Re} [V_I R \exp \{j((\omega + 2\beta V_p)t - \beta x + \theta_0)\}] . \quad (53)$$

This result shows the reflected voltage has a constant frequency different from the frequency of the incident voltage; thus the desired traveling envelope could also be obtained by replacing the termination with a signal

generator having a frequency  $\omega + 2\beta V_p$ . In view of the practical difficulties associated with designing a time-varying impedance, the use of a second signal source is a more favorable technique, and the use of a non-constant impedance will not be considered further.

To obtain the general form of the voltage distribution along a transmission line fed at both ends, consider the configuration shown in Fig. 17. The input impedances of the signal sources will be assumed equal to the characteristic impedance of the line so as to eliminate reflections at the sources.

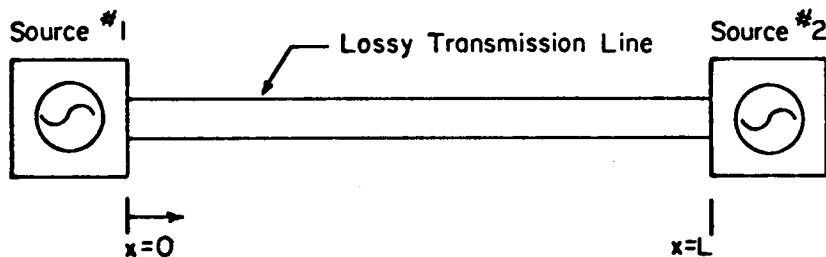


Fig. 17--Two-source method of generating traveling envelope.

The voltages due to sources 1 and 2 respectively are

$$v_1(x,t) = \text{Re} [V_1 \exp \{j(\omega_1 t - \beta_1 x) - \alpha x\}] \quad (54a)$$

$$v_2(x,t) = \text{Re} [V_2 \exp \{j(\omega_2 t + \beta_2 (x-L) + \psi) + \alpha (x-L)\}] \quad (54b)$$

where

- $V_1, V_2$  = magnitude of source voltages
- $\omega_1, \omega_2$  = frequencies of source voltages
- $\beta_1, \beta_2$  = phase constants
- $\psi$  = arbitrary phase difference between sources at  $t = 0$
- $\alpha$  = signal attenuation per unit length due to radiation

and resistive losses

L = length of transmission line.

For convenience, define

$$\omega = \frac{\omega_1 + \omega_2}{2}, \quad (55a)$$

and

$$\Delta\omega = \frac{\omega_1 - \omega_2}{2}, \quad (55b)$$

thus,

$$\omega_1 = \omega + \Delta\omega \quad (56a)$$

and

$$\omega_2 = \omega - \Delta\omega. \quad (56b)$$

The phase constants are defined as

$$\beta_1 = \frac{\omega_1}{V_{p1}},$$

$$\beta_2 = \frac{\omega_2}{V_{p2}},$$

where

$V_{p1}, V_{p2}$  = phase velocity of signals 1 and 2 respectively.

Assuming the transmission line is nondispersive, i.e., phase velocity is independent of frequency, then

$$V_{p1} = V_{p2},$$

and

$$\beta_1 = \beta + \Delta\beta \quad (57a)$$

$$\beta_2 = \beta - \Delta\beta \quad (57b)$$

where

$$\beta = \frac{\omega}{V_{p1}} = \frac{\omega}{V_{p2}}$$

$$\Delta\beta = \frac{\Delta\omega}{V_{p1}} = \frac{\Delta\omega}{V_{p2}}.$$

Substituting Eqns. (56) and (57) for  $\omega_1, \beta_1$  in Eqn. (54) and applying the principle of superposition, the total voltage along the line is obtained

$$v(x,t) = \text{Re} [V_1 \exp \{j(\omega t - \Delta\beta x)\} \exp \{-\alpha x + j(\Delta\omega t - \beta x)\} \\ + V_2 \exp \{-\alpha L\} \exp \{j(\omega t - \Delta\beta x)\} \exp \{\alpha x - j(\Delta\omega t - \beta x + 2\theta)\}] \quad (58)$$

where

$$\theta = \frac{1}{2} [(\beta - \Delta\beta) L - \psi].$$

To simplify Eqn. (58), it is convenient to define two constants C and  $\gamma$  such that

$$C \exp \{-\gamma\} = V_1 \quad (59a)$$

and

$$C \exp \{\gamma\} = V_2 \exp \{-\alpha L\}. \quad (59b)$$

Substituting Eqns. (59a) and (59b) for the respective terms in Eqn. (58), one obtains after some algebraic manipulation

$$v(x,t) = \text{Re} [C \exp \{j(\omega t - \Delta\beta x - \theta)\} [\exp \{-\gamma - \alpha x + j(\Delta\omega t - \beta x + \theta)\} \\ + \exp \{\gamma + \alpha x - j(\Delta\omega t - \beta x + \theta)\}] ] \quad (60)$$

Noting that

$$\exp \{j\gamma\} = \cos \gamma + j \sin \gamma,$$

the real part of Eqn. (60) is obtained

$$v(x,t) = C [\cos (\omega t - \Delta\beta x - \theta) \exp \{-\gamma - \alpha x\} \cos (\Delta\omega t - \beta x + \theta) \\ - \sin (\omega t - \Delta\beta x - \theta) \exp \{-\gamma - \alpha x\} \sin (\Delta\omega t - \beta x + \theta) \\ + \cos (\omega t - \Delta\beta x - \theta) \exp \{\gamma + \alpha x\} \cos (\Delta\omega t - \beta x + \theta) \\ + \sin (\omega t - \Delta\beta x - \theta) \exp \{\gamma + \alpha x\} \sin (\Delta\omega t - \beta x + \theta)] \quad (61)$$

Using the definitions of the hyperbolic functions

$$\cosh (y) = \frac{\exp \{y\} + \exp \{-y\}}{2}$$

and

$$\sinh (y) = \frac{\exp \{y\} - \exp \{-y\}}{2} ,$$

one obtains for Eqn. (61)

$$v(x, t) = 2C [\cosh (\gamma + \alpha x) \cos (\Delta \omega t - \beta x + \theta) \cos (\omega t - \Delta \beta x - \theta) + \sinh (\gamma + \alpha x) \sin (\Delta \omega t - \beta x + \theta) \sin (\omega t - \Delta \beta x - \theta)]. \quad (62)$$

However, the expression for the voltage given by Eqn. (62) is simply the trigonometric expansion of an amplitude- and phase-modulated carrier, thus

$$v(x, t) = g(x, t) \cos (\omega t - \Delta \beta x - \phi(x, t) - \theta) \quad (63)$$

where

$$g(x, t) = 2C [\sinh^2 (\gamma + \alpha x) + \cos^2 (\Delta \omega t - \beta x + \theta)]^{1/2},$$

$$\phi(x, t) = \tan^{-1} [\tanh (\gamma + \alpha x) \tan (\Delta \omega t - \beta x + \theta)],$$

$$\tanh ( ) = \sinh ( ) / \cosh ( ) = \text{hyperbolic tangent.}$$

To obtain the desired traveling signal, consider  $v^2(x, t)$  and note that the low-pass component is

$$1/2 g^2(x, t) = \frac{4C^2}{2} [\sinh^2 (\gamma + \alpha x) + 1/2 \cos 2(\Delta \omega t - \beta x + \theta) + 1/2]. \quad (64)$$

The phase velocity of the propagating component of  $g^2(x, t)$  is

$$\frac{dx}{dt} = V_R = \frac{\Delta \omega}{\beta} . \quad (65)$$

Note that the velocity of  $g^2(x, t)$  may be made arbitrarily small by reducing the frequency difference between the signal generators shown in

Fig. 16. Also, when  $\Delta\omega = 0$ , a standing wave (zero velocity) is obtained as would be expected. A more convenient form of the phase velocity is

$$V_A = \frac{\Delta f}{f} V_0 \quad (66)$$

where

$V_0$  = propagation velocity of a TEM wave on the transmission line  $\approx$  velocity of light

$$\Delta f = \Delta\omega/2\pi$$

$$f = \omega/2\pi.$$

A simple receiver capable of recovering the low-velocity reference signal is shown in Fig. 18. If the receiver were stationary, the output of the band-pass filter would be

$$h(x,t) = 2C^2 \cos 2(\Delta\omega t - \beta x + \theta). \quad (67)$$

However, note that if the receiver were moving with velocity  $V$ , there would be an additional time-varying term in  $g^2(x, t)$

$$g_a(t) = 2C^2 \sinh^2(\gamma + \alpha Vt).$$

To estimate the frequency of  $g_a(t)$ , it is convenient to expand the hyperbolic sine function

$$g_a(t) = 2C^2 \left[ \frac{\exp\{2(\gamma + \alpha Vt)\} - 2 + \exp\{-2(\gamma + \alpha Vt)\}}{4} \right]. \quad (68)$$

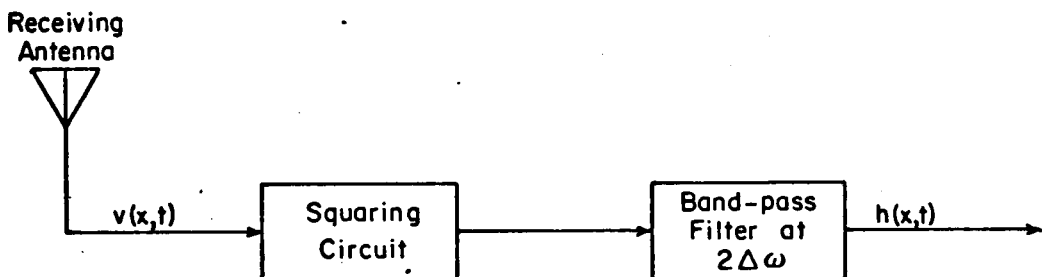


Fig. 18--Basic receiver required to recover reference signal.

The Fourier Transform of Eqn. (68) is

$$G_q(\omega) = \frac{C^2}{2} \left[ \frac{\exp\{2\gamma\}}{j\omega - 2\alpha V} + \frac{\exp\{-2\gamma\}}{j\omega + 2\alpha V} - 2\delta(\omega) \right], \quad (69)$$

and for

$$\omega \neq 0,$$

one obtains

$$G_q(\omega) = -C^2 \frac{j\omega \cosh(\gamma) + 2\alpha V \sinh(\gamma)}{\omega^2 + (2\alpha V)^2}.$$

The asymptotic spectrum of  $G_a(\omega)$  is shown in Fig. 19. Clearly, for

$$\omega > 20\alpha V,$$

there is no significant contribution to the spectrum of  $g^2(x, t)$ .

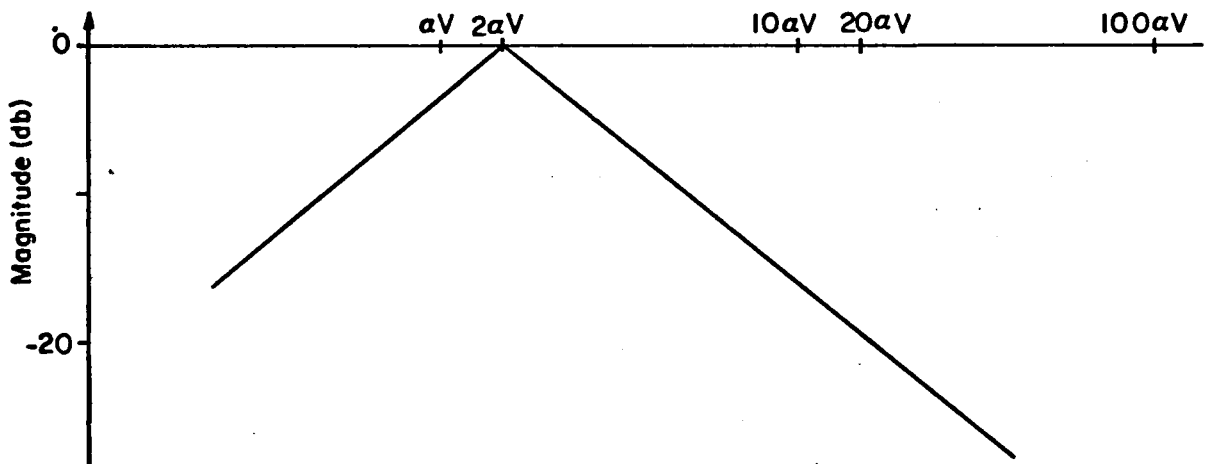


Fig. 19--Asymptotic spectrum of  $G_a(\omega)$ .

Assuming a rather large value of 10 db/100ft<sup>†</sup> for the line attenuation,  $\alpha$ ,

<sup>†</sup>Decibal (db) values are defined as

$$\alpha_{db} = 20 \log_{10}(\alpha)$$

and a velocity of 100 ft/sec, then the cut-off frequency of  $g_a(t)$  would be

$$\begin{aligned}\omega_c &= 20\alpha V \\ &= 20(\sqrt{10}/100) \cdot 100 \\ &\approx 63 \text{ rad/sec}.\end{aligned}$$

Thus, even though it is implied by Eqn. (65) that the phase velocity could be arbitrarily small, for the case of a moving receiver,  $2\Delta\omega$  must be sufficiently larger than  $\omega_c$  to allow recovery of  $h(x, t)$  as suggested in Fig. 17.

Assuming the restriction on  $\Delta\omega$  is satisfied, the output of the band-pass filter in Fig. 17 would be given by Eqn. (67) whether or not the receiver were moving

$$h(x, t) = 2C^2 \cos 2(\Delta\omega t - \beta x + \theta).$$

Solving Eqns. (59a) and (59b) for the constant  $C^2$ , one obtains

$$C^2 = V_1 V_2 \exp\{-\alpha L\}.$$

and assuming equal signals from the two sources,

$$h(x, t) = 2V_M^2 \exp\{-\alpha L\} \cos 2(\Delta\omega t - \beta x + \theta) \quad (70)$$

where

$$V_M = V_1 = V_2.$$

It is interesting to note that the amplitude of  $h(x, t)$  is independent of  $x$ , although the amplitude of the received signal,  $v(x, t)$ , could vary considerably as a function of  $x$ . Also note that an estimate of the allowable line length could be determined from the receiver sensitivity, signal power, and line attenuation. This point will be considered further in the next chapter.

Recall that the assumed reference signal used in the development

of Chapter II was

$$s(x, t) = B \sin(\omega_R t - \beta_R x).$$

Comparing this expression with  $h(x, t)$  given by Eqn. (70) one obtains

$$B = \sqrt{2} V_R \exp\{-\alpha L/2\}, \quad (71a)$$

$$\omega_R = 2 \Delta \omega, \quad (71b)$$

$$\beta_R = 2 \beta, \quad (71c)$$

$$\theta = -\pi/4. \quad (71d)$$

The reference signal wavelength defines the minimum vehicle spacing and is given by

$$\lambda_R = \frac{2\pi}{\beta_R} = \frac{\pi}{\beta},$$

but

$$\beta = \frac{2\pi}{\lambda}$$

where

$$\lambda = \frac{V_0}{f} = \text{wavelength of the carrier frequency of } v(x, t)$$

thus

$$\lambda_R = \frac{1}{2} \lambda. \quad (72)$$

This result shows that the velocity of the reference signal and the wavelength may be varied independently since from Eqn. (66) the velocity is proportional to the frequency difference and the wavelength is determined by the average frequency. To illustrate this point, consider a vehicle spacing ( $\lambda_R$ ) of 100 ft, then from Eqn. (68)

$$\lambda = 200 \text{ ft},$$

and assuming  $V_0 = \text{speed of light} \approx 10^9 \text{ ft/sec}$ , the carrier frequency is

$$f = 5 \text{ MHz}.$$

To obtain a phase velocity of  $1/1000$  the speed of light, one finds from Eqn. (66)

$$\Delta f = \frac{f}{1000}$$

or

$$\Delta f = 5 \text{ KHz.}$$

Therefore, the source frequencies required are

$$f_1 = f + \Delta f = 5.005 \text{ MHz}$$

and

$$f_2 = f - \Delta f = 4.995 \text{ MHz}$$

This technique for slowing down the reference signal is a promising solution to the problem of maintaining adequate time-synchronization among several sampling units. In the next section, the performance of this method in the presence of frequency errors, such as caused by oscillator frequency drift, will be investigated.

#### D. Sensitivity Analysis

In addition to the position uncertainty introduced by the previously discussed synchronization error, there is also a reference velocity error due to deviations in the sampling frequency,  $f_s$ , and the source frequencies,  $f_1$  and  $f_2$ . From Eqn. (16), the command velocity is

$$V_R^* = \frac{\omega_R - k\omega_s}{\beta_R}$$

Substituting for  $\omega_R$  and  $\beta_R$  as given by Eqns. (71b) and (71c), one obtains

$$V_R^* = \frac{2\Delta\omega - k\omega_s}{2\beta}$$

or equivalently

$$V_R^* = \lambda \left( \Delta f - \frac{kf_s}{2} \right). \quad (73)$$

In any practical system, it will not be possible to maintain 100% accuracy of the parameters  $\lambda$ ,  $f_s$ , and  $\Delta f$ . To examine the sensitivity

of  $V_R^*$  to variations in these parameters, consider the total differential of  $V_R^*$

$$d(V_R^*) = \frac{\partial V_R^*}{\partial \lambda} d(\lambda) + \frac{\partial V_R^*}{\partial f_s} d(f_s) + \frac{\partial V_R^*}{\partial \Delta f} d(\Delta f) \quad (74)$$

where

$d( )$  = total differential

$\frac{\partial( )}{\partial( )}$  = partial derivative.

The partial derivatives are easily found from Eqn. (73)

$$\frac{\partial V_R^*}{\partial \lambda} = \Delta f - \frac{k f_s}{2} = \frac{V_R^*}{\lambda}, \quad (75)$$

$$\frac{\partial V_R^*}{\partial f_s} = -\frac{k \lambda}{2} = \frac{V_R^* - \lambda \Delta f}{f_s}, \quad (76)$$

$$\frac{\partial V_R^*}{\partial \Delta f} = \lambda = \frac{\lambda \Delta f}{\Delta f} \quad (77)$$

From Eqn. (66)

$$V_R = \frac{\Delta f}{f} V_0$$

or

$$V_R = \lambda \Delta f \quad (78)$$

since

$$\lambda = V_0 / f,$$

and the partial derivatives given by Eqns. (76) and (77) are

$$\frac{\partial V_R^*}{\partial f_s} = \frac{V_R^* - V_R}{f_s}, \quad (79)$$

$$\frac{\partial V_R^*}{\partial \Delta f} = \frac{V_R}{\Delta f}. \quad (80)$$

Substituting Eqns. (75), (79), and (80) for the respective terms in Eqn.

(74), one obtains

$$\frac{dV_R^*}{V_R^*} = \frac{d\lambda}{\lambda} + \left(1 - \frac{V_R}{V_R^*}\right) \frac{df_s}{f_s} + \frac{V_R}{V_R^*} \frac{d(\Delta f)}{\Delta f}. \quad (81)$$

Noting that  $dV_R^*/V_R^*$  represents a small percent or relative variation in  $V_R^*$ , one sees that relative errors in  $f_g$  and  $\Delta f$  are magnified by the factor  $V_R/V_R^*$ . Since  $V_R$  can be arbitrarily controlled, the logical solution would be to make  $V_R$  as small as possible. However,  $V_R$  is not independent of  $\Delta f$  and the sensitivity of  $V_R^*$  with respect to  $\Delta f$  is the same, regardless of the value of  $V_R$ . To prove this point, one obtains from Eqn. (66)

$$\frac{V_R}{\Delta f} = \frac{V_0}{f}$$

and from the definitions of  $\Delta f$  and  $f$ , it follows that

$$\frac{V_R}{V_R^*} \frac{d(\Delta f)}{\Delta f} = \frac{V_0}{V_R^*} \frac{d(f_1 - f_2)}{f_1 + f_2}.$$

Recalling that

$$\frac{\Delta f}{f} < \frac{1}{1000}$$

to obtain the required time synchronization, one sees that

$$f_1 \approx f_2$$

and

$$\frac{V_R}{V_R^*} \frac{d(\Delta f)}{\Delta f} \approx \frac{V_0}{V_R^*} \left( \frac{df_1}{2f_1} - \frac{df_2}{2f_2} \right). \quad (82)$$

Since  $f_1$  and  $f_2$  are generated by essentially identical sources, it is convenient to define the source frequency error as

$$\frac{df_g}{f_g} \approx \frac{df_1}{f_1} \approx \frac{df_2}{f_2}$$

where

$$f_g = \text{either of the frequencies } f_1 \text{ or } f_2.$$

Also, since the sources are independent, the maximum value of the error term in Eqn. (82) would be

$$\begin{aligned} \left[ \frac{df_1}{2f_1} - \frac{df_2}{2f_2} \right]_{\max} &= \left| \frac{df_1}{2f_1} \right| + \left| \frac{df_2}{2f_2} \right| \\ &\approx \frac{df_g}{f_g}, \end{aligned}$$

thus, for the worst case

$$\frac{V_R}{V_R^*} \frac{d(\Delta f)}{\Delta f} \approx \frac{V_0}{V_R^*} \frac{df_s}{f_s} \quad (83)$$

Using

$$V_R^* = 100 \text{ ft/sec,}$$

then

$$\frac{V_0}{V_R^*} \approx 10^7$$

and to maintain less than a 1% contribution to the velocity error due to errors in  $f_1$  and/or  $f_2$ , regardless of the value of  $V_R$ , there is an inherent accuracy requirement of  $10^{-7}\%$  for the source frequencies. Thus, even though reducing the value of  $V_R$  decreases the effect of variations in  $f_s$ , the stringent stability requirements on  $f_1$  and  $f_2$  rules out a straightforward implementation of the technique described in the previous section. However, note from Eqn. (81) that an error in  $f_s$  results in an essentially opposite error in  $V_R^*$  as does an error in  $\Delta f$ . This suggests that if  $f_s$  were derived from  $\Delta f$ , then any error in  $\Delta f$  would be at least partially compensated for by the corresponding error in  $f_s$ . To examine this possibility, let  $f_s$  be a constant multiple of the difference frequency

$$f_s = r \Delta f$$

where

$$r = \text{frequency conversion gain.}$$

Then the error in  $f_s$  is

$$\frac{df_s}{f_s} = \frac{dr}{r} + \frac{d(\Delta f)}{\Delta f} \quad (84)$$

Note that the term  $dr/r$  represents the error associated with the technique

used to generate  $f_g$ . Substituting Eqn. (84) in Eqn. (81), one obtains

$$\frac{dV_R^*}{V_R^*} = \frac{d\lambda}{\lambda} + \frac{d(\Delta f)}{\Delta f} + \left(1 - \frac{V_R}{V_R^*}\right) \frac{dr}{r}. \quad (85)$$

From Eqn. (83)

$$\frac{d(\Delta f)}{\Delta f} = \frac{V_o}{V_R} \frac{df_g}{f_g},$$

and from the definition of the carrier wavelength

$$\lambda = \frac{V_o}{f} = \frac{V_o}{\frac{1}{2}(f_1 + f_2)} \approx \frac{V_o}{f_g}$$

one obtains

$$\frac{d\lambda}{\lambda} = - \frac{df_g}{f_g},$$

thus, upon substituting the above terms in Eqn. (85),

$$\frac{dV_R^*}{V_R^*} = \left(\frac{V_o}{V_R} - 1\right) \frac{df_g}{f_g} + \left(1 - \frac{V_R}{V_R^*}\right) \frac{dr}{r}. \quad (86)$$

Note that it is not possible to simultaneously minimize both error terms in Eqn. (86). The accuracy requirements for  $f_g$  and  $r$  necessary to maintain less than 1% contribution to the velocity error from each parameter are shown in Fig. 20 as a function of phase velocity reduction ( $V_R/V_o$ ). This figure clearly shows that, in order to reduce the required accuracy of the source frequencies, one must be able to generate a correspondingly more accurate frequency ratio ( $r = f_g/\Delta f$ ). As will be shown in the following section, it seems certain that the required accuracy for  $r$  can be obtained.

#### E. A Technique for Generating $f_g$

With the present state of the art in digital electronics, it is possible to obtain highly accurate frequency ratios. It is suggested that

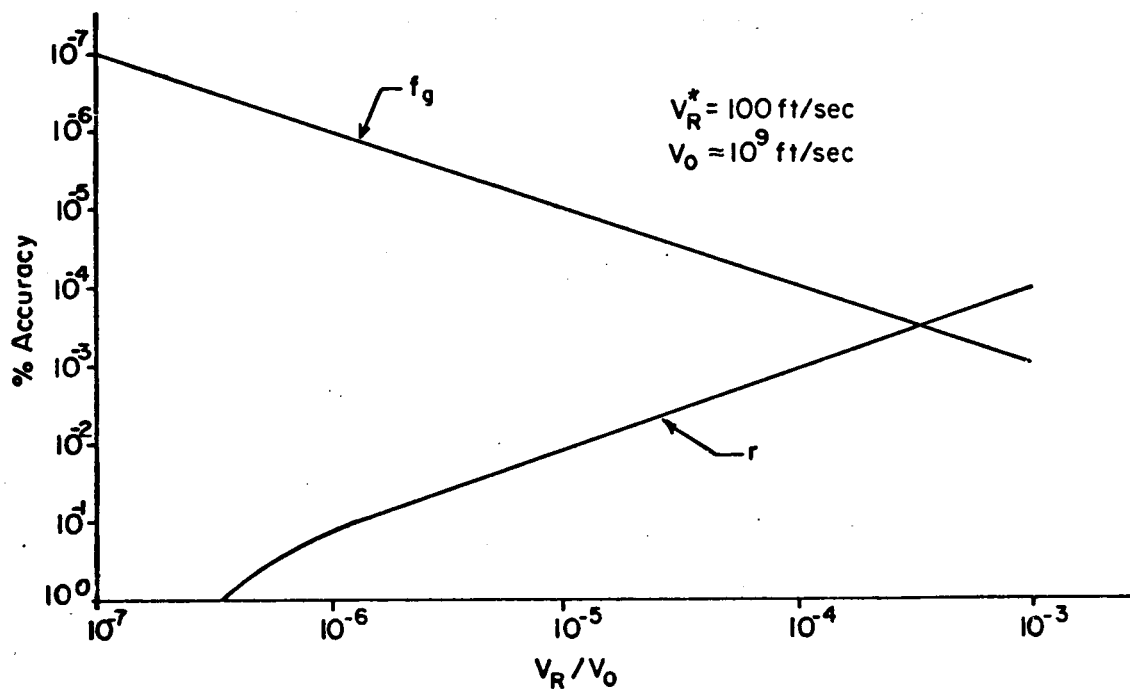


Fig. 20--Accuracy required of  $f_g$  and  $r$  to maintain less than 1% velocity error from each parameter.

a technique similar to that used in digital frequency synthesizers<sup>13</sup> could be used to generate  $f_s$  as shown in Fig. 21.

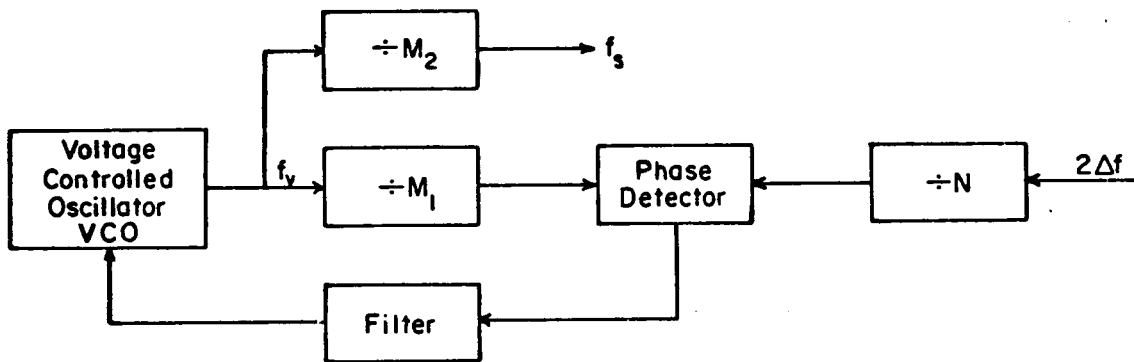


Fig. 21--Digital frequency synthesizer.

Note that the input is shown as  $2\Delta f$ . This is required since standard mixing of  $f_1 = f + \Delta f$  and  $f_2 = f - \Delta f$  produces an output of  $2\Delta f$ , not  $\Delta f$ .

The phase detector controls the VCO such that its output ( $f_v$ ) is

$$\frac{f_v}{M_1} = \frac{2\Delta f}{N}$$

As shown in Fig. 19

$$f_s = \frac{f_v}{M_2}$$

thus

$$f_s = \frac{2M_1}{M_2 N} \Delta f$$

By a proper choice of the digital counters (dividers), any specified frequency ratio may be obtained:

$$\frac{f_s}{\Delta f} = r = \frac{2M_1}{M_2 N} \quad (87)$$

The required value of  $r$  is obtained from Eqn. (73) with  $f_s = r\Delta f$ :

$$V_R^* = \lambda \Delta f \left(1 - \frac{kr}{2}\right) \quad (88)$$

thus

$$r = \frac{2}{k} \left(1 - \frac{V_R^*}{V_R}\right) \quad (89)$$

since

$$V_R = \lambda \Delta f$$

Choosing

$$\frac{V_R^*}{V_R} = 10^{-3}$$

to minimize the accuracy requirement of  $f_g$  as shown in Fig. 20, then for

$$V_R^* = 100 \text{ ft/sec}$$

$$\frac{V_R^*}{V_R} = 10^{-4}$$

and

$$r = \frac{2}{k} (.9999) .$$

From Eqn. (87), the counters must be chosen such that

$$\frac{M_1}{M_2 N} = \frac{9999}{k 10,000} . \quad (90)$$

Since there are an essentially unlimited number of solutions to this equation, one must carefully examine the operation of the circuit shown in Fig. 21 to obtain the best choice for the counter values.

Note from Fig. 20, that for the assumed phase velocity ( $v_R/v_o = 10^{-3}$ ), the required accuracy for the frequency ratio ( $r$ ) is  $10^{-4}\%$ . Assuming  $\Delta f$  is exact, then from Eqn. (84), the error in  $f_s$  is

$$\delta f_s = \frac{dr}{r} f_s$$

where

$$\delta f_s = \text{magnitude of the error in } f_s$$

and

$$\delta f_s = 10^{-6} f_s \quad (91)$$

for

$$\frac{dr}{r} = 10^{-4} \% .$$

One sees from Fig. 21 that, assuming ideal operation of the digital counters, an error in  $f_s$  implies a corresponding frequency error ( $f_e$ ) at the phase detector input

$$f_e = \frac{M_2}{M_1} \delta f_s .$$

If the frequency error were introduced at time  $t = 0$ , then the phase error would be

$$\phi_e(t) = 2\pi \frac{M_2}{M_1} \delta f_s t .$$

From Eqn. (90)

$$\frac{M_2}{M_1} \approx \frac{k}{N},$$

thus

$$\phi_e(t) \approx 2\pi \frac{k}{N} \delta f_s t. \quad (92)$$

To interpret Eqn. (92) easily, it is advantageous to express the phase error in terms of the equivalent time error. Note from Fig. 21 that the period of the phase detector reference signal is

$$T = \frac{N}{2\Delta f},$$

thus

$$\phi_e(t) = 2\pi \frac{t_e}{T} = 2\pi \frac{(2\Delta f)}{N} t_e \quad (93)$$

where

$t_e$  = time error in seconds.

Equating Eqns. (92) and (93), one obtains

$$t_e = \frac{k}{(2\Delta f)} \delta f_s t. \quad (94)$$

To increase the sensitivity of the VCO control loop, one would wish to have the time error increase as rapidly as possible. Recall from Chapter II, that

$$k = \left[ \frac{\omega_R}{\omega_s} \right]$$

where

$[ ]$  = greatest integer function

thus

$$k = \left[ \frac{2\Delta f}{f_s} \right].$$

On the basis of Eqn. (94) alone, one would choose a large value of  $k$ , and hence a lower sampling rate. However, as will be shown later,  $k$  should be

unity, thus

$$t_e = \frac{\delta f_s}{2\Delta f} t \quad (95)$$

As shown in the previous section, for

$$\lambda = 200 \text{ ft}$$

and

$$\frac{V_R}{V_0} = 10^{-3} ,$$

then

$$\Delta f = 5 \text{ KHz} .$$

With  $k = 1$ , then

$$f_s \approx 2\Delta f = 10 \text{ KHz} ,$$

and from Eqn. (91)

$$\delta f_s \approx 10^{-2} \text{ Hz} .$$

Using the above values of  $\Delta f$  and  $\delta f_s$  in Eqn. (95), one obtains

$$t_e \approx 10^{-6} t . \quad (96)$$

Considering the present technology of digital electronics, it is not unreasonable to presume that time-synchronization of two pulse trains accurate within 1 to 10 nanoseconds could be easily achieved. Choosing

$$t_e < 10^{-8} \text{ sec.}$$

to be conservative, then from Eqn. (96)

$$t < 10^{-2} \text{ sec} .$$

This result implies that a  $10^{-4}\%$  error in  $f_s$ , and hence the same error in  $r$ , would exist for at most 10 milliseconds. Clearly, an accuracy of at least  $10^{-4}\%$  could be maintained by the circuit shown in Fig. 21.

Since it is expected that the proposed method for generating  $f_s$  will provide the required steady-state accuracy, it is necessary to con-

sider the transient response due to random disturbances. Note from Fig. 21 that the frequency of the reference signal at the phase detector is

$$f_{\phi} = \frac{2 \Delta f}{N} .$$

Due to the use of digital signals, phase information is available only at switching instants as shown in Fig. 22.

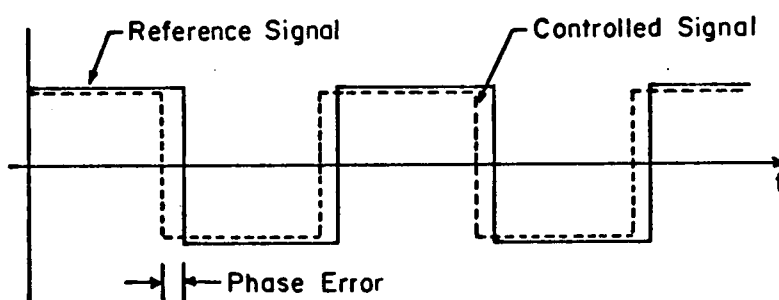


Fig. 22--Two pulse trains showing phase error.

Thus, to increase the phase-information rate, or equivalently, closed-loop response time, one should use a large value for  $f_{\phi}$ ; hence,  $N$  should be unity, and

$$f_{\phi} = 2 \Delta f \quad (97)$$

If large phase errors are introduced, the controlled frequency could skip one or more cycles in returning to a steady-state, phase-locked operating point. This phenomena is shown schematically in Fig. 23. Note from Fig. 21 that the phase of the VCO output after the controlled signal has skipped one cycle is

$$\phi_v(t) = M_i (2\pi + \phi_R(t))$$

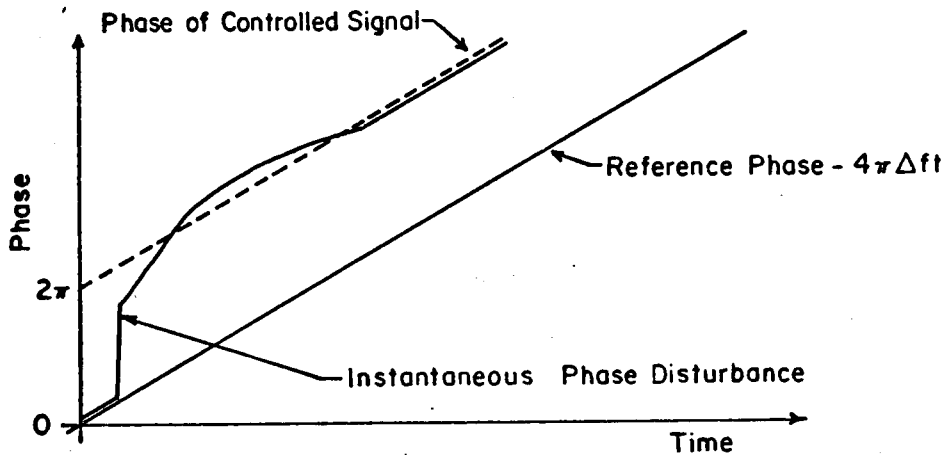


Fig. 23--Cycle skipping of controlled signal due to large phase disturbance.

where

$$\phi_R(t) = 4\pi\Delta ft = \text{reference phase.}$$

The phase of the sampling signal is

$$\begin{aligned} \phi_s(t) &= \frac{\phi_v(t)}{M_2} \\ &= 2\pi \frac{M_1}{M_2} + \frac{M_1}{M_2} \phi_R(t) . \end{aligned}$$

The term

$$\frac{M_1}{M_2} \phi_R(t)$$

represents the desired phase of  $f_s$ , while the phase-error introduced by the skipped cycle is

$$\phi_{se}(t) = 2\pi \frac{M_1}{M_2} .$$

As shown by Eqn. (93), the equivalent time error is

$$t_{se} = \frac{M_1}{M_2} T_s \quad (98)$$

where

$$T_s = \frac{1}{f_s} = \text{period of sampling signal.}$$

The effect of this time error is shown in Fig. 24.

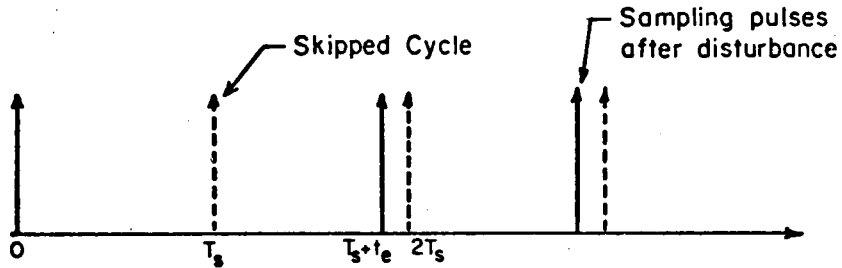


Fig. 24--Sampling time error due to skipped pulses.

As shown in this figure, the sampling pulses after the skipped cycle are offset from the desired pulse train by an amount

$$\delta t = T_s - t_{se}$$

From Eqn. (98), this time error is

$$\delta t = T_s \left( \frac{M_2 - M_1}{M_2} \right). \quad (99)$$

The effect of this time error is to introduce a vehicle position error as given by Eqn. (48)

$$\delta x = V_R \delta t$$

where

$$\begin{aligned} V_R &= \text{velocity of reference signal} \\ &\approx 10^6 \text{ ft/sec} \end{aligned}$$

thus, from Eqn. (99)

$$\delta x \approx 10^6 T_s \left( \frac{M_2 - M_1}{M_2} \right). \quad (100)$$

Clearly, to minimize the effect of cycle-skipping, one must choose  $M_2$  nearly

equal to  $M_1$ . From Eqn. (90), with the previous result  $N = 1$ ,

$$\frac{M_1}{M_2} = \frac{9999}{10,000} \frac{1}{k} .$$

With  $k = 1$ , then

$$M_1 = 9999$$

and

$$M_2 = 10\,000.$$

For  $k = 1$ ,

$$f_s \approx 2 \Delta f = 10 \text{ KHz} , \quad (101)$$

and from Eqn. (100)

$$\delta_x \approx 100 \left( \frac{1}{10\,000} \right) = 0.01 \text{ ft.}$$

It is obvious that several cycles could be skipped during a transient disturbance in the VCO control loop without seriously affecting the vehicle reference position. Note that this result justifies the earlier use of  $k = 1$ .

It is important to note that the effect of a random change in the counter  $M_2$  has not been considered in the previous analysis. Inasmuch as  $M_2$  would be a "free-running" counter, there is essentially no ideal method to detect and/or correct random errors there. As a reasonable solution to this problem, a form of majority-logic, as shown in Fig. 25, could be used. The output of the majority-logic control would be

$$f_s = \begin{cases} f_{s_1} , f_{s_1} \text{ synchronized with } f_{s_2} \text{ and/or } f_{s_3} \\ f_{s_2} , f_{s_2} \text{ synchronized with } f_{s_3} \text{ only} \end{cases}$$

The reset control is required to return the counters to a synchronized state when an error is detected. Note that it has been implicitly assumed

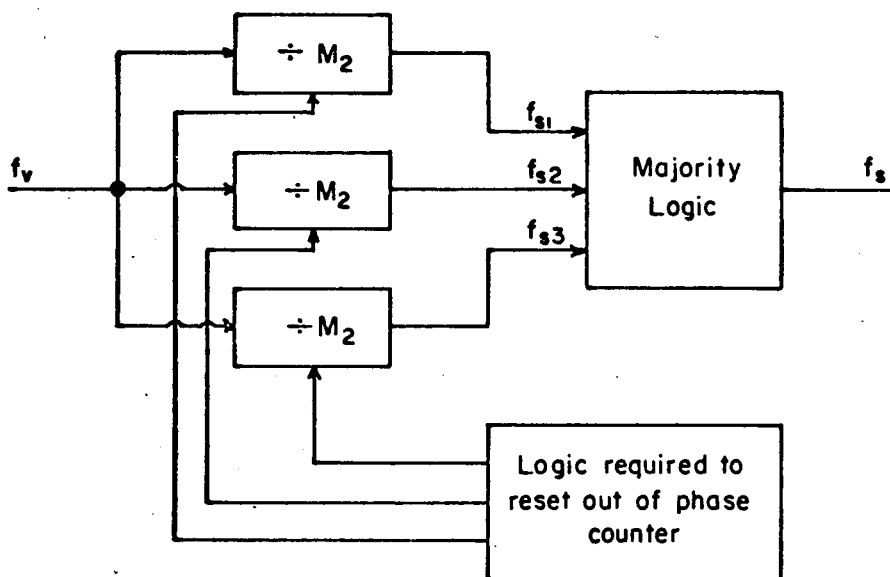


Fig. 25--Majority-logic generation of  $f_s$ .

that the probability of errors occurring in two counters simultaneously is negligible.

It has been shown by the analyses presented in this section and the preceding section, that one can be reasonably confident of overcoming the practical problems associated with the design of the proposed system for generating the required reference signals. In the next section, the response of a vehicle due to transient errors in the reference signal will be examined.

#### F. Considerations of the Effects of Transient Errors in the Reference Signal

The command velocity error is given by Eqn. (81), and considering an error in  $f_s$  only, one obtains

$$\delta V_R^* \approx -V_R \frac{\delta f_s}{f_s}$$

where

$\delta V_R^*$  = command velocity error

$\delta f_s$  = sampling frequency error.

Using

$$f_s \approx 10 \text{ KHz ,}$$

$$V_R \approx 10^6 \text{ ft/sec ,}$$

as obtained in the previous sections

$$\delta V_R^* \approx -100 \delta f_s .$$

Recall from Chapter II, that the vehicle control signal is (see Eqn. (28))

$$f_i(t) = \frac{B}{T_s} \sin \left( \beta_R \int_0^t e(\tau) d\tau \right)$$

where

$e(\tau)$  = vehicle velocity error.

Since

$$e(t) = V_R^* - V(t) ,$$

an error in  $V_R^*$  would introduce an apparent vehicle velocity error of magnitude

$$e(t) = -100 \delta f_s ,$$

for which the corresponding vehicle control signal would be

$$f_i(t) = \frac{B}{T_s} \sin \left( \beta_R (-100 \delta f_s t) \right) .$$

Assuming an inter-vehicle spacing of 100 ft,

$$\beta_R = \frac{2\pi}{100}$$

and

$$f_i(t) = -\frac{B}{T_s} \sin (2\pi \delta f_s t) .$$

For a relatively small error in  $f_s$ , say 1%,

$$\begin{aligned}\delta f_s &\approx (0.01)(10 \text{ kHz}) \\ &\approx 100 \text{ Hz}.\end{aligned}$$

If the time constant of the vehicle control system were about 2 sec, as shown in Chapter II, then the vehicle could not respond to the above error ( $\omega \approx 600 \text{ rad/sec}$ ) and the only effect would be a temporary loss of position control. Since the vehicle would be in an essentially uncontrolled mode for this situation, it would be necessary that the control loop shown in Fig. 21 have a relatively fast response in regaining phase-lock to correct  $f_s$ . An uncontrolled situation for as long as 10 seconds might be tolerable, though certainly undesirable.

If the frequency error in  $f_s$  were much smaller, for example,

$$\delta f_s = 1 \text{ Hz},$$

then

$$f_s(t) = -\frac{B}{T_s} \sin(2\pi t),$$

and the vehicle would be able to respond to the apparent velocity error. However, note that for this case the percent error in  $f_s$  would be

$$\frac{\delta f_s}{f_s} = 10^{-2} \%.$$

and hence the control loop in Fig. 21 would be very near phase-lock. It seems reasonable to assume that an error of this magnitude would be corrected very rapidly and that the vehicle would experience only a minor disturbance.

The reader should bear in mind that the above heuristic arguments are intended only to provide an intuitive feel for the expected vehicle response due to transient errors in  $V_R^*$ . Until actual experience

with the circuit of Fig. 21 is obtained, one cannot be certain of the severity of the above problem.

In addition to transient errors in  $V_R^*$ , there is a position uncertainty introduced by phase-jitter in the sampling frequency. This is an inherent problem associated with digital techniques and is magnified in the present application due to the VCO control loop as shown in Fig. 21. To examine the effect of this phase-jitter, let the  $n^{\text{th}}$  sampling instant be

$$t_n = nT_s + \tilde{t}_p$$

where

$nT_s$  = expected sampling instant

$\tilde{t}_p$  = random time error.

Recall from Chapter II that ideal sampling of the reference wave produces the output (see Eqn. (7))

$$f(t) = \sum_{n=-\infty}^{\infty} B \sin(n\omega_R T_s) \delta(t - nT_s).$$

In the presence of phase-jitter, this result must be modified such that

$$f(t) = \sum_{n=-\infty}^{\infty} B \sin(\omega_R(nT_s + \tilde{t}_p)) \delta(t - nT_s - \tilde{t}_p)$$

Assuming a priori that the variance of  $\tilde{t}_p$  must be extremely small, then one can, as a first-order approximation, adequately represent  $f(t)$  as

$$f(t) \approx \sum_{n=-\infty}^{\infty} [B \sin(n\omega_R T_s) + B \omega_R \tilde{t}_p] \delta(t - nT_s).$$

Note that in the above form, the effect of  $\tilde{t}_p$  is equivalent to a noise component associated with the reference signal. It is not unreasonable to assume that  $\tilde{t}_p$  is a narrow-band random process centered at  $f_s$ . With this assumption, the entire noise component would be passed by the low-

pass filter used to recover the error signal, thus

$$f_i(t) = \frac{B}{T_s} \sin\left(\beta_R \int_0^t e(z) dz\right) + \frac{B}{T_s} \omega_R \tilde{T}_P \quad (102)$$

To examine the effect of the noise term, it is convenient to compare the vehicle control system with the classical phase-locked loop. To this end, note that Fig. 10 may be rearranged as shown in Fig. 26.

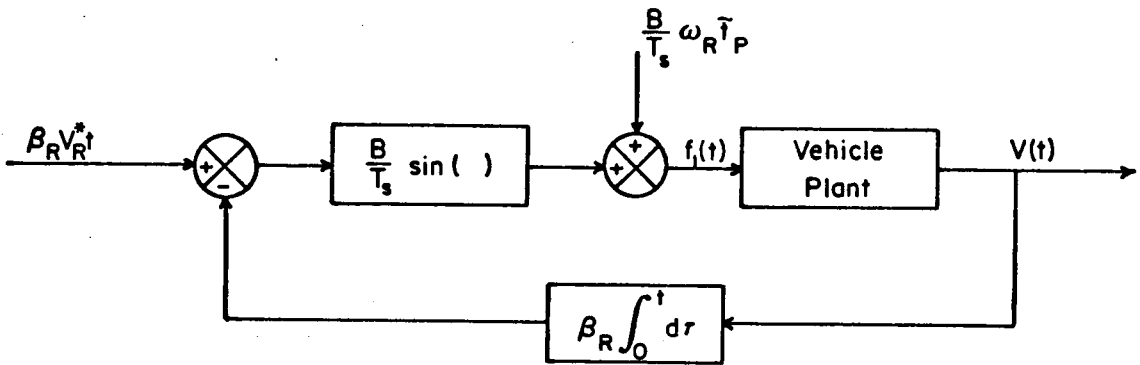


Fig. 26--Alternate model of vehicle control system with noise term.

Note that under steady-state operating conditions, the vehicle velocity ( $V(t)$ ) is controlled such that its phase (position) is equal to the reference phase (position). Clearly, this control system is analogous to a phase-locked loop.

Viterbi<sup>15</sup> has shown that the variance of the phase error for a first-order loop is

$$\sigma_\phi^2 = \frac{N_o B_L}{A^2} \quad (103)$$

where

$N_o B_L$  = noise power

$A^2$  = received signal power.

The analogous parameters in Fig. 24 are

$$\sigma_{\phi}^2 = \text{Var} \left\{ \beta_R \int_0^t (V_R^* - V(\tau)) d\tau \right\},$$

$$N_0 B_L = \left( \frac{B}{T_s} \omega_R \right)^2 \text{var} \{ \tilde{\epsilon}_p \},$$

and

$$A^2 = \frac{1}{2} \left( \frac{B}{T_s} \right)^2,$$

where

$\text{var} \{ \}$  = variance of a random variable.

Note that

$$\int_0^t (V_R - V(\tau)) d\tau = \text{position error} = X_e,$$

thus

$$\sigma_{\phi}^2 = \beta_R^2 \text{var} \{ X_e \},$$

and from Eqn. (103)

$$\text{var} \{ X_e \} = \frac{2\omega_R^2}{\beta_R^2} \text{var} \{ \tilde{\epsilon}_p \}. \quad (104)$$

Since, (see Eqn. (71))

$$\beta_R = \frac{2\pi}{\lambda_R} = \frac{4\pi}{\lambda}$$

and

$$\omega_R = 2\pi f_R = 4\pi \Delta f,$$

one can simplify Eqn. (104) to obtain

$$\sigma_{X_e} = \sqrt{2} \lambda \Delta f \sigma_{\tilde{\epsilon}_p} \quad (105)$$

where

$\sigma$  = standard deviation.

Noting that

$$\lambda \Delta f = V_R \approx 10^6$$

and neglecting the constant  $\sqrt{2}$ , then

$$\sigma_{x_e} \approx 10^6 \sigma_{t_p}. \quad (106)$$

To obtain an estimate of  $\sigma_{t_p}$ , recall that it was maintained that the VCO control loop shown in Fig. 21 could achieve a time-synchronization in the order of 1 - 10 nanoseconds. As shown in this figure, the phase error appearing at the phase detector is

$$\phi_e = \frac{\delta \phi_v}{M_1}$$

where

$\delta \phi_v$  = phase error in VCO output.

Since the phase of the sampling frequency is

$$\phi_s = \frac{\phi_v}{M_2}$$

where

$\phi_v$  = VCO phase,

the phase error in the sampling frequency is

$$\begin{aligned} \delta \phi_s &= \frac{\delta \phi_v}{M_2} \\ &= \frac{M_1}{M_2} \phi_e. \end{aligned}$$

As was shown earlier

$$M_1 \approx M_2,$$

thus

$$\delta \phi_s \approx \phi_e. \quad (107)$$

From Eqn. (97), the frequency of the signal at the phase-detector would be

$$f_{\phi} = 2\Delta f ,$$

and from Eqn. (101), the sampling frequency would be

$$f_s \approx 2\Delta f ,$$

thus, since the frequencies are nearly equal, it is implied by Eqn. (107) that

$$t_p \approx t_e$$

where

$t_e$  = pulse synchronization error at the phase detector.

Assuming  $t_e$  is in the order of 1 - 10 nanoseconds, then

$$\sigma_{t_p} \approx \sigma_{t_e} \approx 10^{-8}$$

Thus, from Eqn. (106)

$$\sigma_{x_e} \approx 10^{-2} \text{ ft.}$$

Assuming the circuit shown in Fig. 21 can maintain a steady-state pulse synchronization within 10 nanoseconds, one can be reasonably sure that the phase-jitter introduced by the digital techniques will have a negligible effect on the vehicle position.

### G. Summary

A novel technique for generating the reference signals for a synchronous longitudinal vehicle control system has been presented in this chapter. Although there are rather severe frequency and synchronization requirements, on the basis of the detailed, theoretical analysis presented, it appears that the major practical problems associated with this technique can be overcome. However, much experimental work will be required to vali-

date these results.

Some of the basic system requirements necessary to implement this technique in an automated highway system will be considered in the next chapter.

CHAPTER IV  
AN OVERVIEW OF BASIC SYSTEM DESIGN

A. Introduction

An analysis of one possible technique for synchronous longitudinal control of automated vehicles and a proposed method for implementing this technique have been presented in the previous chapters. In this chapter, some of the basic requirements for the design of the proposed system will be considered.

B. Transmission Line Considerations

As described in the preceding chapter, the reference signal required for the proposed system is obtained from the interference pattern of two signals transmitted along a transmission line. Some of the major problems expected to be encountered in the design of this transmission system are:

1. Specifying the maximum allowable length of cable between sources.
2. Controlling the reference signal such that it appears to be continuous at a junction of two adjacent links.

To examine the first of these, recall from Chapter III that the envelope of the interference pattern is (see Eqn. (63))

$$g(x, t) = 2C [\sinh^2(\gamma + \alpha x) + \cos^2(\Delta\omega t - \beta x + \theta)]^{1/2}$$

The constants C and  $\gamma$ , obtained from Eqn.s (59a) and (59b), are

$$C = [V_1 V_2]^{1/2} \exp\{-\alpha L/2\}$$

$$\gamma = -\alpha L/2 + \ln(V_2/V_1).$$

Assuming both sources have equal signal strength, then

$$C = V_m \exp\{-\alpha L/2\},$$

$$\gamma = -\alpha L/2,$$

where

$$V_M = V_1 = V_2$$

and

$$g(x, t) = 2 V_m \exp\{-\alpha L/2\} [\sinh^2(\alpha x - \frac{\alpha L}{2}) + \cos^2(\Delta\omega t - \beta x + \theta)]^{1/2}. \quad (108)$$

Near the center of the line ( $x = L/2$ ), the peak amplitude of the envelope ( $G_M$ ) is

$$G_M \approx 2 V_m \exp\{-\alpha L/2\} \quad (109)$$

and the amplitude of the signal received onboard a vehicle is

$$R_m = \eta_T G_M \quad (110)$$

where

$R_M$  = amplitude of signal received near  $x = L/2$ ,

$\eta_T$  = transmission efficiency.

Note that the transmission efficiency is a function of:

1. Transmission line design ( $\eta_T = 0$  for coaxial cable).
2. Vehicle receiving antenna.
3. Transmission line to antenna spacing.

For a specified receiver sensitivity,†  $R_s$ , then

$$R_m > R_s$$

for adequate signal strength, and from Eqns. (109) and (110)

$$2 \eta_T V_m \exp \{-\alpha L\} > R_s \quad (111)$$

Solving Eqn. (111) for L, one obtains

$$L_{max.} = \frac{2}{\alpha} [\eta_T' + V_m' - R_s' + 6] \quad (112)$$

where

- $L_{max}$  = maximum line length in feet
- $\alpha$  = line attenuation in db/ft
- $\eta_T', V_m', R_s'$  = db values of  $\eta_T$ ,  $V_m$ , and  $R_s$  respectively
- 6 =  $20 \ln 2$  db.

Since  $\eta_T$  and  $R_s$  are fixed for any given transmission line, receiver combination, it would appear that the maximum line length is limited only by the amount of signal power available ( $1/2V_M^2$ ). However, inasmuch as the proposed system would radiate R-F energy, all applicable Federal Communications Commission restrictions would have to be satisfied. Maximum radiation would occur near either end of the line segment; thus, for a given transmission system, the source power would be limited by the radiation level near  $x = 0$ .

Another factor effecting the maximum line length, is the relative change in amplitude with position along the line. However, discussion of this effect will be deferred until the next section.

---

†Receiver sensitivity is defined as the minimum input signal required to give a standard output.

The second major objective in the design of the transmission system is to provide a continuous reference signal at the junction of two links, as shown in Fig. 27. The signals in each link are

$$\begin{aligned}
 V_A(x,t) &= V(x,t) , & 0 < x < L \\
 V_B(x,t) &= V(x-L,t) , & L < x < 2L \\
 g_A(x,t) &= g(x,t) , & 0 < x < L \\
 g_B(x,t) &= g(x-L,t) , & L < x < 2L
 \end{aligned}
 \tag{113}$$

where

$V_A, V_B$  = total voltage in links A and B respectively

$g_A, g_B$  = envelope of voltage.

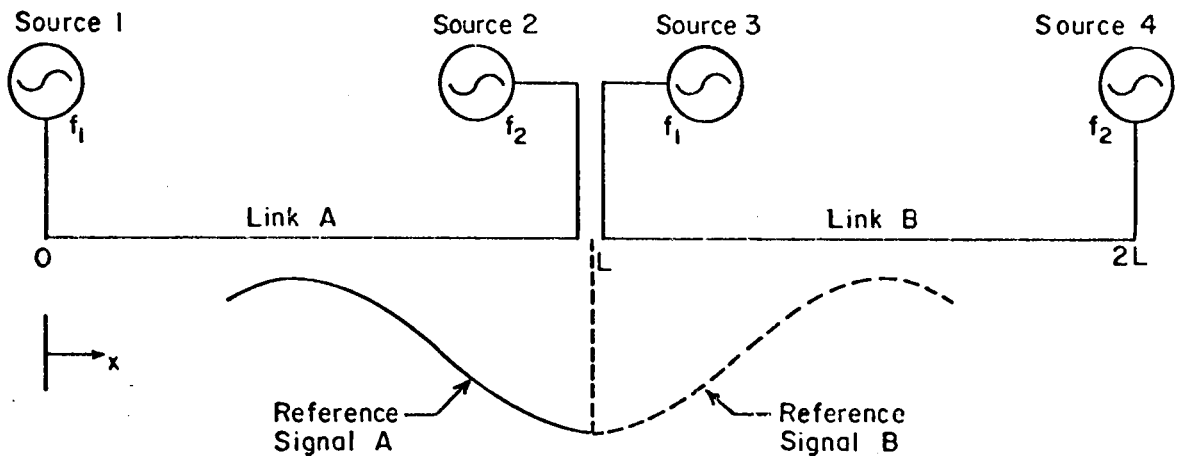


Fig. 27--Two adjacent transmission links.

Since the reference signal is obtained from the envelope, it is only necessary to provide continuity of  $g(x, t)$  at  $x = L$ . From Eqns. (108) and (113)

$$g_A(L, t) = 2 V_m \exp \left\{ -\alpha \frac{L}{2} \right\} \left[ \sinh^2 \left( \frac{\alpha L}{2} \right) + \cos^2 (\Delta \omega t - \beta L + \theta_A) \right]^{1/2}$$

and

$$g_B(L, t) = 2 V_m \exp \left\{ -\alpha \frac{L}{2} \right\} \left[ \sinh^2 \left( -\frac{\alpha L}{2} \right) + \cos^2 (\Delta \omega t + \theta_B) \right]^{1/2}$$

Since

$$\sinh^2 (y) = \sinh^2 (-y) ,$$

the required continuity at  $x = L$  could be obtained if

$$\theta_B = \theta_A - \beta L . \tag{114}$$

Thus, one possible method to ensure continuity of  $g(x, t)$  would be to control the phase of Source 3 (see Fig. 27) such that Eqn. (114) is satisfied. However, in view of the extreme sensitivity of the reference signal due to changes in the source frequencies, as shown in the preceding chapter, it is unlikely that continuous control of the phase of Source 3 would be feasible. It is suggested that a more practical approach would be to provide separate sampling signals in links A and B. (This approach is outlined in Fig. 28). Note that the envelope in link B has an arbitrary phase with respect to that in link A. As shown in this figure, receiver A detects the reference signal using the sampling pulses for link A, while receiver B uses the pulses for link B. By properly adjusting the phase (time delay) of the pulses in link B, both receivers would produce the same output. Note that it would probably not be possible to use continuous phase control of the sampling signal in link B due to the stringent accuracy requirements developed earlier. However, it is believed that some type of threshold control, as shown in Fig. 29, would be adequate. Vehicle response to step position errors and safety aspects would have to be considered in specifying the allowable tolerance before cor-

reactive action is taken.

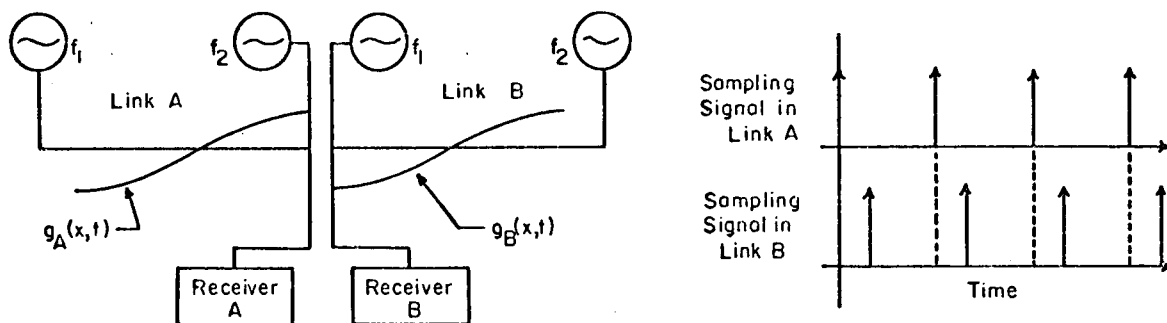


Fig. 28--Technique to provide continuity of  $g(x, t)$  using separate sampling signals.

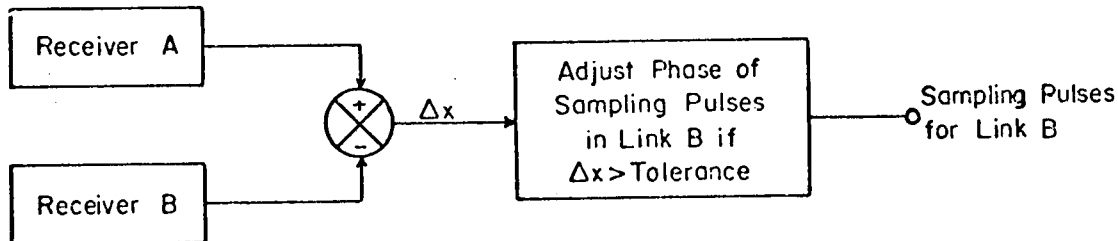


Fig. 29--Threshold control of sampling pulses.

Since the sampling pulses and reference signal must be transmitted to the vehicle via radiation from the transmission line, a severe interference problem could exist at the junction of the two links. Some type of shielding, as suggested in Fig. 30, could reduce this problem; however, it might prove necessary to disable the receiver until the vehicle is past the region of interference.

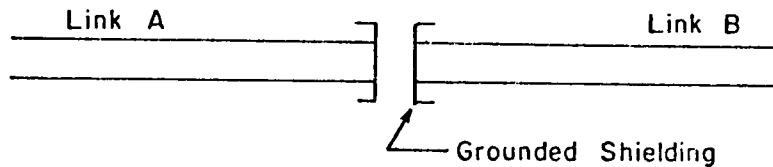


Fig. 30--Shielding at junction of two transmission line links.

It should be noted that, although only two links have been considered here, the technique described is applicable for all succeeding links. This is possible since only the sampling pulses for link B are varied, not pulses in both links simultaneously, to obtain the necessary continuity of the reference signal. Thus, the sampling pulses for a third link would be controlled with respect to link B only, and similarly for all following links.

### C. Receiver Considerations

As shown in Chapter III, the position reference signal would be obtained by demodulating the AM signal

$$V(x,t) = g(x,t) \cos(\omega t - \Delta\beta x + \phi(x,t) - \theta) \quad (63)$$

The desired reference signal would be the band-pass component at  $2\Delta\omega$  of the squared-signal

$$\frac{1}{2} g^2(x,t) = \lambda C^2 [\sinh^2(\gamma + \alpha x) + \frac{1}{2} \cos 2(\Delta\omega t - \beta x + \theta) + \frac{1}{2}].$$

Either square-law detection of  $V(x, t)$  or linear demodulation and squaring the envelope could be used to obtain  $g^2(x, t)$ . However, regardless of the technique used, the important point to note is that the modulation index

$M(x)$  of  $V(x, t)$  varies with position

$$V(x, t) = 2C [\sinh^2(\gamma + \alpha x) + 1/2]^{1/2} [1 + M(x) \cos \lambda(\Delta \omega t - \beta x + \theta)]^{1/2} \cdot \cos(\omega t - \Delta \beta x + \phi(x, t) - \theta)$$

where

$$M(x) = \frac{1}{1 + 2 \sinh^2(\gamma + \alpha x)}$$

Since

$$\gamma = -\alpha L/2,$$

then at

$$x = L/2$$

$$\begin{aligned} \sinh(\gamma + \alpha x) &= \sinh(-\alpha L/2 + \alpha L/2) \\ &= 0, \end{aligned}$$

and

$$M(x) = 1,$$

thus, near the center of the line, the signal is essentially 100% modulated.

However, the modulation index approaches zero near either end of the line

$$\begin{aligned} M(0) = M(L) &= \frac{1}{1 + 2 \sinh^2(-\alpha L/2)} \\ &\approx 2 \exp\{-\alpha L\}, \quad \alpha L \gg 1. \end{aligned}$$

For adequate signal reception in the presence of noise, the modulation index must be greater than some minimum value depending upon the type of demodulation used, thus

$$M(0) > M_{\min}$$

where

$M_{\min}$  = minimum allowable modulation index

and from above

$$L < \frac{1}{\alpha} \ln(M_{min}).$$

With the results from the previous section, one sees that the maximum transmission line length would be determined by satisfying the following constraints:

1. Adequate signal strength at  $x = L/2$ .
2. Source power low enough to satisfy FCC requirements.
3. Adequate modulation index at  $x = 0$  and  $x = L$ .

If the third point were the limiting factor, then one must take full advantage of the state of the art in signal processing to obtain an optimum receiver system.

In addition to the reference signal, the receiver must also demodulate the sampling signal. Since the position reference is transmitted as a very narrow-band signal ( $\frac{\Delta f}{f} < \frac{1}{1000}$ ), the sampling signal could be transmitted very easily along the same line, at a carrier frequency sufficiently large, say  $10f$ . With this approach, the basic receiver structure would be as shown in Fig. 31.

Note that, due to the signal processing required, there would be a time delay from reception at the antenna to the points labeled A and B. It is imperative that these delays be essentially equal, since any difference between them would introduce an uncertainty in vehicle position. To emphasize this point, let

$$\tau_A = \text{delay of the sampling signal}$$

$$\tau_B = \text{delay of the reference signal}$$

then the sampling pulse train ( $P_T(t)$ ) would be

$$P_T(t) = \sum_{-\infty}^{\infty} \delta(t - nT_s - \tau_A)$$

and the sampled reference signal would be

$$f(t) = P_T(t) \cdot s(x, t - \tau_B)$$

$$= \sum_{-\infty}^{\infty} s(x, nT_s + \tau_A - \tau_B) \delta(t - nT_s - \tau_A)$$

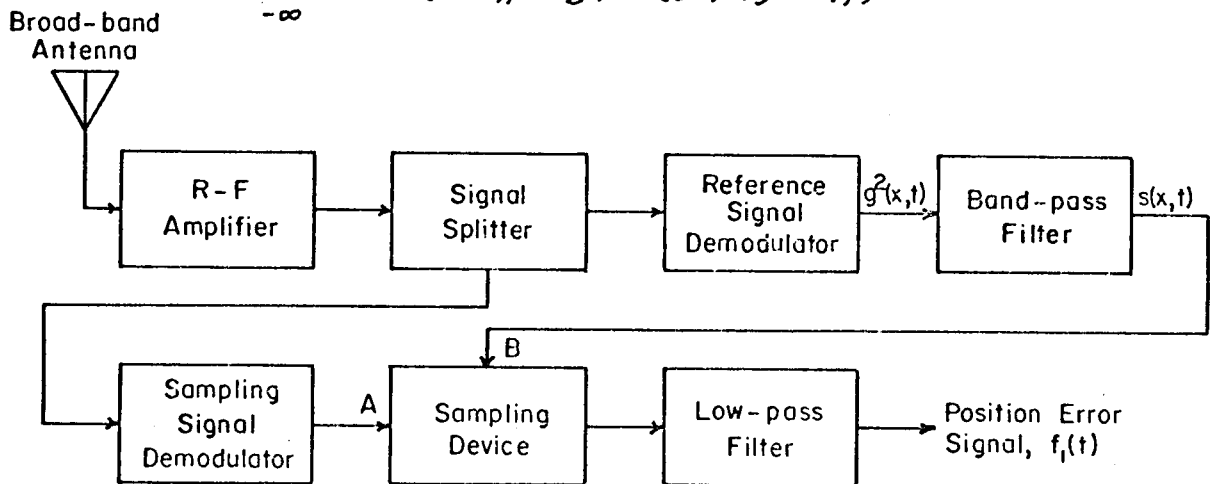


Fig. 31--Basic receiver required.

Recalling that

$$s(x, t) = B \sin(\omega_R t - \beta_R x),$$

then

$$s(x, nT_s + \tau_A - \tau_B) = B \sin \left[ n \omega_R T_s - \beta_R \left( x - \frac{\omega_R}{\beta_R} (\tau_A - \tau_B) \right) \right].$$

Note that the factor

$$\frac{\omega_R}{\beta_R} (\tau_A - \tau_B)$$

represents a position error introduced by the difference in time delays.

Since the phase velocity of the reference wave

$$V_R = \frac{\omega_R}{\beta_R} = \frac{\Delta \omega}{\beta}$$

would be about  $10^6$  ft/sec, this difference in time delay must be less than 1  $\mu$ sec, to avoid severe position uncertainties.

#### D. Traffic Flow Considerations

One of the fundamental requirements of any automated highway system is the capability to change vehicle velocity and headway separation. Recall from Chapter II, that for synchronous longitudinal control, velocity and separation are related by

$$\frac{V_a}{h_a} = \frac{V_b}{h_b}$$

For the proposed system, this constraint could be easily satisfied. The command velocity is given by Eqn. (88)

$$V_R^* = \lambda \Delta f \left(1 - \frac{kr}{2}\right)$$

and vehicle separation is

$$h_R = \lambda_R = \frac{1}{2} \lambda,$$

thus

$$\frac{V_R^*}{h_R} = 2 \Delta f \left(1 - \frac{kr}{2}\right)$$

Note that if  $\Delta f$  and  $r$  were constant, then velocity and separation could be varied by changing the carrier wavelength,  $\lambda$ , while maintaining the required constant velocity-separation ratio. Since

$$\omega_R = 2 \Delta \omega = 4\pi \Delta f,$$

and

$$f_s = 2r \Delta f,$$

this technique of changing  $V_R^*$  and  $h_R$  has an important advantage in that the onboard signal-processor would operate at the same frequencies, even though the velocity command changed.

It is important to note that, the velocity command can only be changed in increments rather than continuously, since the velocity must be constant along any single section of transmission line. Thus, a desired constant deceleration could be approximated as shown in Fig. 32. As an alternative to this technique, it might be possible to let individual vehicles decelerate at a pre-assigned rate until synchronous "phase-lock" could be re-acquired, as shown in Fig. 33. However, deviations of individual vehicle decelerations could lead to large uncertainties in inter-vehicle separation near the region of velocity change.

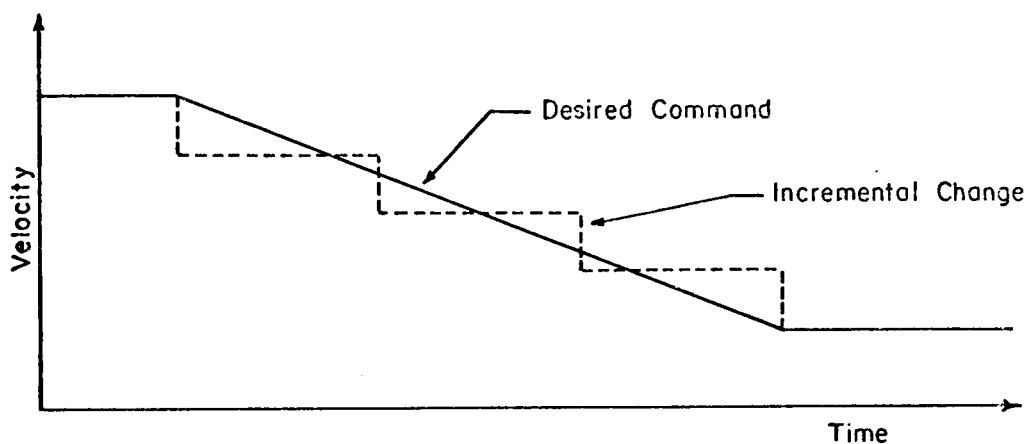


Fig. 32--Approximation to constant deceleration.

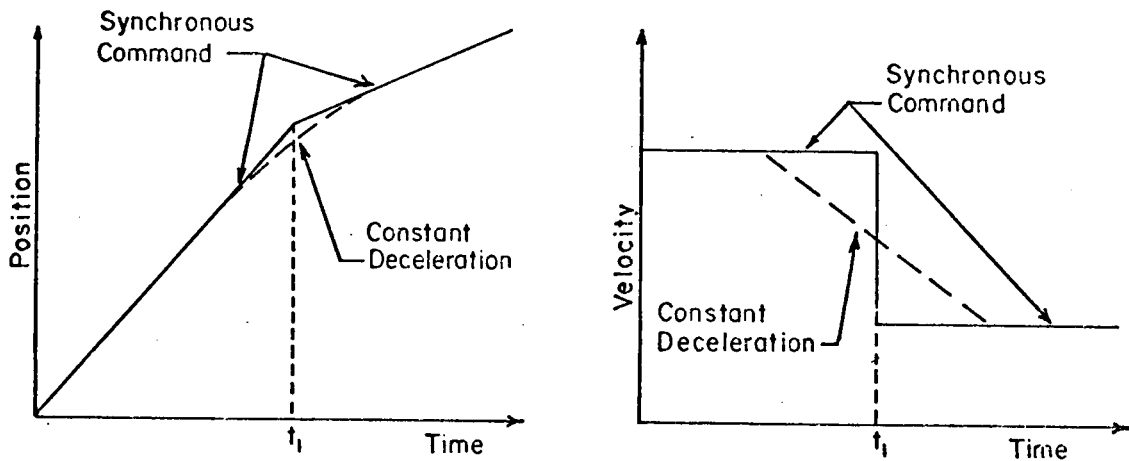


Fig. 33--Non-synchronous deceleration.

#### E. Summary

Some of the more important items that must be considered in the design of the proposed longitudinal control system have been presented in this chapter, namely:

1. Length of transmission line segment, which will be a primary factor in specifying the required roadside equipment.
2. Onboard radio receiver, which will determine how accurately a vehicle can track the reference signal.
3. Command velocity changes such that the velocity-headway constraint of synchronous control is satisfied.

It is not believed that either of the first two considerations will present a major problem in the design of the proposed system. The third point is merely an inherent characteristic of synchronous control in general, and, as was shown, could be easily satisfied by the proposed system.

CHAPTER V  
SUMMARY AND CONCLUSIONS

It appears that considerable improvements in high-speed, high-density traffic flow can be achieved through highway automation. The potential advantages of such automation are increased highway capacity, greater passenger safety, reduced driver effort and increased driver convenience.

One of the subsystems required for any conceivable automated highway scheme, would be one for the longitudinal control of vehicles. Two general approaches to such control have thus far been advocated -- asynchronous control and synchronous control.

This thesis deals with the analysis of a technique for generating the reference signals required for a synchronous longitudinal control scheme. The primary advantages of synchronous control, as given in Chapter I, are:

1. Elimination of instability problems associated with controlling a string of vehicles.
2. Simplification of the problem of merging two strings of vehicles.

However, under synchronous control, individual vehicles have no information about the "state" of other nearby vehicles; therefore, some form of secondary control system must be available to detect emergency situations.

The basic properties of synchronous control and some possible

techniques for implementing it were considered. The method, proposed in this thesis, involves the use of a traveling sinusoidal wave and sampling pulses to provide the necessary vehicle control signal.

A detailed analysis of the proposed technique was presented and it was determined that, in theory, the system is feasible. However, it was found that there would be severe, though not insoluble, practical difficulties associated with this technique and that a great deal of work remains to be done in developing an operational system. This includes the following:

1. The time-synchronization error among individual vehicle sampling units must be minimized.
2. The frequency accuracy of the signal sources must be "high"; therefore, techniques to minimize or eliminate long-term oscillator frequency drift should be examined.
3. A thorough experimental investigation of the proposed method for generating the sampling signal should be performed.
4. A transmission line with adequate radiation and line-loss characteristics should be developed.
5. The relative merits of various possible detection systems (e.g., square-law versus linear detection plus squaring) should be investigated.
6. A vehicle-borne antenna capable of receiving both the reference and sampling signals must be developed.

7. A critical investigation of the suggested techniques for allowing velocity changes should be performed.

It seems likely that all of the expected problems associated with the proposed system can be solved. If so, it would appear that an excellent system for the longitudinal control of vehicles will result.

## REFERENCES

1. Automobile Facts and Figures-1970, Automobile Manufacturers Association.
2. Turner, F. C., "Moving People on Urban Highways," Traffic Quarterly, Volume 24, Number 3, July 1970.
3. Bender, J. G., and Fenton, R. E., "On the Flow Capacity of Automated Highways," Transportation Science, Volume 4, Number 1, February 1970.
4. Bender, J. G., and Fenton, R. E., "A Study of Automatic Car Following," IEEE Trans. on Vehicular Technology, Volume VT-18, Number 3, November 1969.
5. Weiss, E. M., "A Control System for Capsule Transportation," presented at the 20th Annual Conference of the Vehicular Technology Group of the IEEE, Columbus, Ohio, December 1969.
6. TRW Systems Group, "Study of Synchronous Longitudinal Guidance as Applies to Intercity Automated Highway Networks," Final Report prepared for The Office of High Speed Transportation, Department of Transportation, September 1969.
7. Godfrey, M. B., "Merging in Automated Transportation Systems," PhD. Thesis, Department of Mechanical Engineering, Massachusetts Institute of Technology, June 1968.
8. Wilkie, D. F., "A Moving Cell Control Scheme for Automated Transportation Systems," Transportation Science, Volume 4, Number 4, November 1970.
9. Plotkin, S. C., "Automation of the Highways, an Overview," IEEE Trans. on Vehicular Technology, Volume VT-18, Number 2, August 1969.
10. TRW Systems Group, "Automated Highway Systems," April 1970. (PB191696)
11. Papoulis, A., The Fourier Integral and its Applications, McGraw-Hill Book Company, 1962.
12. Bender, J. G., and Fenton, R. E., "On Vehicle Longitudinal Dynamics," presented at the 5th International Symposium on the Theory of Traffic Flow and Transportation, Berkeley, California.
13. "Studies in Vehicle Automatic Longitudinal Control," Communication and Control Systems Laboratory, The Ohio State University, Columbus, Ohio, Report EES-276A, April 1969.

14. Reference Data for Radio Engineers, International Telephone and Telegraph Corporation, 4th Edition, 11th Printing, December 1964.
15. Viterbi, A., Principles of Coherent Communications, McGraw-Hill Book Company, 1966.